

8-6-1999

Regulation of F-actin binding to platelet moesin in vitro by both phosphorylation of threonine 558 and polyphosphatidylinositides

F. Nakamura

L. Huang

Kersi N. Pestonjamas

See next page for additional authors

Follow this and additional works at: http://escholarship.umassmed.edu/wfc_pp

 Part of the [Cell Biology Commons](#), and the [Medicine and Health Sciences Commons](#)

Repository Citation

Nakamura, F.; Huang, L.; Pestonjamas, Kersi N.; Luna, Elizabeth J.; and Furthmayr, H., "Regulation of F-actin binding to platelet moesin in vitro by both phosphorylation of threonine 558 and polyphosphatidylinositides" (1999). *Women's Health Research Faculty Publications*. Paper 301.

http://escholarship.umassmed.edu/wfc_pp/301

This material is brought to you by eScholarship@UMMS. It has been accepted for inclusion in Women's Health Research Faculty Publications by an authorized administrator of eScholarship@UMMS. For more information, please contact Lisa.Palmer@umassmed.edu.

Regulation of F-actin binding to platelet moesin in vitro by both phosphorylation of threonine 558 and polyphosphatidylinositides

Authors

F. Nakamura, L. Huang, Kersi N. Pestonjamas, Elizabeth J. Luna, and H. Furthmayr

Rights and Permissions

Citation: Mol Biol Cell. 1999 Aug;10(8):2669-85.

Regulation of F-Actin Binding to Platelet Moesin In Vitro by Both Phosphorylation of Threonine 558 and Polyphosphatidylinositides

Fumihiko Nakamura,* Laiqiang Huang,[†] Kersi Pestonjamas,[‡]
Elizabeth J. Luna,[‡] and Heinz Furthmayr^{†§}

*Laboratory of Environmental Biochemistry, Department of Environmental Biology, Graduate School of Agricultural Sciences, Tohoku University, Sendai 981-8555, Japan; [†]Molecular Mechanisms of Disease Laboratories, Department of Pathology, Stanford University School of Medicine, Stanford, California 94305-5324; and [‡]Department of Cell Biology, University of Massachusetts Medical School, Worcester, Massachusetts 016055

Received March 1, 1999; Accepted June 1, 1999
Monitoring Editor: Thomas D. Pollard

Activation of human platelets with thrombin transiently increases phosphorylation at ⁵⁵⁸threonine of moesin as determined with phosphorylation state-specific antibodies. This specific modification is completely inhibited by the kinase inhibitor staurosporine and maximally promoted by the phosphatase inhibitor calyculin A, making it possible to purify the two forms of moesin to homogeneity. Blot overlay assays with F-actin probes labeled with either [³²P]ATP or ¹²⁵I show that only phosphorylated moesin interacts with F-actin in total platelet lysates, in moesin antibody immunoprecipitates, and when purified. In the absence of detergents, both forms of the isolated protein are aggregated. Phosphorylated, purified moesin co-sediments with α - or β/γ -actin filaments in cationic, but not in anionic, nonionic, or amphoteric detergents. The interaction affinity is high (K_d , ~1.5 nM), and the maximal moesin:actin stoichiometry is 1:1. This interaction is also observed in platelets extracted with cationic but not with nonionic detergents. In 0.1% Triton X-100, F-actin interacts with phosphorylated moesin only in the presence of polyphosphatidylinositides. Thus, both polyphosphatidylinositides and phosphorylation can activate moesin's high-affinity F-actin binding site in vitro. Dual regulation by both mechanisms may be important for proper cellular control of moesin-mediated linkages between the actin cytoskeleton and the plasma membrane.

[§] Corresponding author. E-mail address: hfurthmayr@pathology.stanford.edu.

Abbreviations used: ⁵⁵⁸T-p-moesin, moesin phosphorylated at the ⁵⁵⁸T site; DEAE, diethylaminoethyl; DOTMAC, dodecyltrimethylammonium chloride; KYKpTLR and KYKTLR, phosphorylated and nonphosphorylated peptides; LysoPC:diC12:0, L- α -phosphatidylcholine dilauroyl; LysoPC:C16:0, L- α -phosphatidylcholine dipalmitoyl; mAbMo, monoclonal moesin antibodies; np-moesin, nonphosphorylated moesin; pAbKYKpTLR, affinity-purified polyclonal antibodies specific for phosphorylated moesin; pAbMo, affinity-purified polyclonal moesin antibodies; PGE₁, prostaglandin E₁; PG:diC16, L- α -phosphatidyl-DL-glycerol dipalmitoyl sodium salt; PA:diC16:0, L- α -phosphatidic acid dipalmitoyl sodium salt; PI, L- α -phosphatidylinositol sodium salt; PI(3)P:diC16:0, L- α -phosphatidylinositol 3-phosphate dipalmitoyl; PI(4)P, L- α -phosphatidylinositol 4-phosphate; PI(3,4)P₂:diC16:0, L- α -phosphatidylinositol 3,4-bisphosphate dipalmitoyl; PI(4,5)P₂, L- α -phosphatidylinositol 4,5-bisphosphate; PI(3,4,5)P₃:diC16:0, L- α -phosphatidylinositol 3,4,5-triphosphate dipalmitoyl; PIPx, phosphatidylinositol polyphosphate; PMA, phorbol 12-myristate 13-acetate.

INTRODUCTION

Moesin, ezrin, and radixin have been proposed to function as linkages between the plasma membrane and F-actin in the cortex of cells. Structurally, these proteins are composed of three major regions: an N-terminal domain of ~300 amino acid residues consisting of several discrete subdomains with amino acid sequences that are identical in the three proteins across a wide variety of species, a 150-amino-acid long sequence predicted to form central α -helices, and a short C-terminal domain of ~100 amino acid residues that includes a conserved sequence of ~30 residues at the C-terminal end (Gould *et al.*, 1989; Tsukita *et al.*, 1989; Funayama *et al.*, 1991; Lankes and Furthmayr, 1991; Lankes *et al.*, 1993). Functionally, the N-terminal domain has been associated with binding to membrane constituents, as revealed by its distribution in cellular microextensions, its localization after transfection with DNA expression constructs (Algrain *et al.*, 1993;

Amieva *et al.*, 1998), and its direct interaction with membrane proteins (Hirao *et al.*, 1996; Yonemura *et al.*, 1998), adapter proteins containing the PDZ motif (Reczek *et al.*, 1997; Short *et al.*, 1998), and polyphosphatidylinositides (Niggli *et al.*, 1995). Likewise, binding of the C-terminal domain to actin filaments has been established by co-distribution with stress fibers (Algrain *et al.*, 1993; Amieva *et al.*, 1998) and by *in vitro* binding data with fragments containing the entire domain (Turunen *et al.*, 1994; Pestonjamas *et al.*, 1995; Matsui *et al.*, 1998). F-actin binding studies with full-length native proteins have yielded less consistent results. Earlier work could not demonstrate this activity, but recently, Yao *et al.* (1996) demonstrated high-affinity and preferential binding of ezrin purified from gastric parietal cells to β -actin and suggested that this activity depends on phosphorylation. More recent studies, using *in vitro* phosphorylation by PKC- θ of recombinant and/or partially purified ezrin and moesin, also produced evidence for a phosphorylation-dependent interaction (Pietromonaco *et al.*, 1998; Simons *et al.*, 1998).

N-terminal recombinant fragments of ~300 amino acid residues of ezrin and radixin bind ~100-residue C-terminal fragments (Gary and Bretscher, 1995; Magendantz *et al.*, 1995). This has given rise to the concept that full-length molecules are stabilized by an intramolecular interaction between the two domains.

We recently showed that activation of human platelets with thrombin is associated with a rapid and transient 1.5-fold increase in the phosphorylation of a single threonine residue in position 558 of the moesin sequence (Nakamura *et al.*, 1995). Phosphorylation at this site could be inhibited with the phosphokinase inhibitor staurosporine and maximally enhanced with the phosphatase inhibitor calyculin A. Both treatments were accompanied by characteristic morphological changes of the platelet. Phosphorylation of the same residue was confirmed in other cells in that lysophosphatidic acid treatment of serum-starved Swiss 3T3 cells changed the phosphorylation state of moesin, ezrin, and radixin with similar kinetics (Matsui *et al.*, 1998), as did stimulation of mast cells, macrophages, and NIH3T3 cells (Ichimaru and Furthmayr, unpublished results; Nakamura *et al.*, 1996; Nakamura and Furthmayr, unpublished results). The mechanism for lysophosphatidic acid-stimulated phosphorylation of moesin apparently involved activation of the small GTPase Rho and its downstream kinase, Rho kinase, because Rho kinase efficiently phosphorylated two residues ⁵⁶⁴Thr (⁵⁵⁸Thr in moesin) and ⁵⁷³Thr of a C-terminal fragment of radixin *in vitro*. However, Rho-kinase did not phosphorylate the full-length native protein. Phosphorylation of the C-terminal threonine residues prevented this domain from interacting with the N domain but did not change the inherent F-actin binding ability of the fragment (Matsui *et al.*, 1998). The fact that Rho kinase did not phosphorylate the full-length protein suggested either that a different kinase acts *in vivo* or that additional regulatory steps or factors are necessary.

In the present study we tested the hypothesis that the F-actin binding function of moesin is activated during stimulation of platelets by phosphorylation of the single threonine residue (558Thr) that we had identified earlier. The platelet system allowed us to isolate and purify both the unmodified and phosphorylated cellular form of moesin to

homogeneity for biochemical and functional studies with F-actin blot overlay and co-sedimentation assays. In contrast to reports from other laboratories with recombinant and/or partially purified cellular proteins, we found that both phosphorylation of ⁵⁵⁸Thr and the presence of either polyphosphoinositides or a cationic detergent is required for the F-actin binding activity of moesin. This result suggests a more complex two-step regulatory mechanism for the activation of the high-affinity F-actin binding site.

MATERIALS AND METHODS

Antibodies and Lipids

Mouse monoclonal antibody 38/87 and the affinity-purified polyclonal antibody pAbMo were used for the identification of moesin by immunoblotting and for immunoprecipitation, respectively (Amieva and Furthmayr, 1995). The affinity-purified polyclonal antibodies pAbKYKpTLR and pAbKYKTLR were prepared as described previously (Nakamura *et al.*, 1996). Actin monoclonal antibodies were purchased from Sigma (St. Louis, MO). PG:diC16:0 and PA:diC16:0 were purchased from Wako Pure Chemical Industries (Osaka, Japan). PI(3)P:diC16:0, PI(3,4)P₂:diC16:0 and PI(3,4,5)P₃:diC16:0 were purchased from Matreya (Pleasant Gap, PA). Bovine brain-derived PI(4)P, PI(4,5)P₂ and PI(1,4,5)P₃ were purchased from Boehringer Mannheim (Mannheim, Germany) or Sigma. Other lipids derived from bovine brain, unless noted, were purchased from Sigma. Micelles of PI(3,4)P₂:diC16:0, PI(4,5)P₂:diC16:0, and PI(3,4,5)P₃:diC16:0 were prepared by dissolving in HE (20 mM HEPES-NaOH, pH 7.2, 0.2 mM EGTA, 0.2 mM EDTA) as a stock solution of 1 mg/ml. These lipids were well soluble, whereas other phosphatidylinositol polyphosphates needed to be sonicated. Small unilamellar vesicles were prepared from lipids by sonication in a Branson (Danbury, CT) cup sonicator, intensity setting 5, at 50% duty cycle, for 9 min (3 × 3 min) to a stock solution of 1 mg/ml in HE. Multilamellar vesicles were prepared from lipids as a stock solution of 1 mg/ml in HE as described (Hope *et al.*, 1986).

Isolation and Activation of Platelets in Suspension

Human blood platelets were prepared as described previously (Nakamura *et al.*, 1995). Gel-filtered platelets were resuspended in Tyrode's buffer (136 mM NaCl, 2.9 mM KCl, 12 mM NaHCO₃, 0.36 mM NaH₂PO₄, 1.8 mM CaCl₂, 0.4 mM MgCl₂, 5.5 mM glucose, pH 7.4) at 1 × 10⁹ platelets/ml. Platelets were activated by the addition of 1.0 NIH unit of thrombin/ml, 1 μ M phorbol 12-myristate 13-acetate (PMA), 1 μ M calcium ionophore A23187, or 5 μ M prostaglandin E₁ (PGE₁). For some experiments, platelets were incubated for 10 min with 100 nM calyculin A or 1 μ M staurosporine. All experiments were performed at 37°C.

Gel Electrophoresis and Western Blotting

Platelets were lysed by addition of an equal volume of 2× SDS sample buffer (125 mM Tris-HCl, 4% SDS, 20% glycerol, 10% 2-mercaptoethanol, pH 6.8). Moesin was immunoprecipitated from lysates of platelets as described previously (Nakamura *et al.*, 1995). Polypeptides were separated by SDS-PAGE on a 9.0% polyacrylamide gel under reducing conditions. Phosphorylated (⁵⁵⁸T-p-) or nonphosphorylated (np-) moesin was detected by immunoblotting with affinity-purified pAbKYKpTLR and pAbKYKTLR antibodies and the enhanced chemiluminescence detection system (Amersham, Arlington Heights, IL).

Purification of Phosphorylated and Nonphosphorylated Moesin from Human Platelets

Platelets in Tyrode's buffer were incubated for 10 min at 37°C with 100 nM calyculin A or 1 μ M staurosporine for the isolation of

phosphorylated or unphosphorylated moesin, respectively. The pretreated platelets were then lysed by addition of 10 volumes of buffer A (20 mM Tris-HCl, 0.5 mM EDTA, 0.5 mM EGTA, 10 mM 2-mercaptoethanol, pH 7.5) containing 1% Triton X-100, proteinase inhibitors (100 mg/ml leupeptin, 1 mM PMSF, 100 mM benzamide), and phosphate inhibitors (100 nM calyculin A, 40 mM sodium pyrophosphate, 10 μ M phenyl arsine oxide). After centrifugation at $25,000 \times g$ for 60 min at 4°C, moesin was isolated and purified from the supernatant by several chromatographic steps in the order listed below. All purification procedures were performed at 4°C. During each step, fractions containing phosphorylated and unphosphorylated moesin were identified by immunoblotting with affinity-purified pAbKYKpTLR and pAbKYKTLR antibodies (Nakamura *et al.*, 1996).

Heparin-Agarose Chromatography. The supernatant was loaded onto a heparin-agarose column (15 \times 57 mm, Sigma, St. Louis, MO), pre-equilibrated with buffer B (buffer A containing 1 mM PMSF and 40 mM sodium pyrophosphate), and developed with a 200-ml linear gradient of 0–500 mM NaCl in the equilibrating buffer at a flow rate of 1 ml/min. Fractions, containing np-moesin (72–92 ml) or ⁵⁵⁸T-p-moesin (100–116 ml), were pooled and diluted 1:2 with buffer B.

Blue-Sepharose Chromatography. The pooled fractions from step 1 were loaded onto a blue-Sepharose CL-6B fast flow column (15 \times 57 mm; Pharmacia, Piscataway, NJ), preequilibrated with buffer B. Moesin was eluted with a linear salt gradient (200 ml) from 0 to 800 mM NaCl in buffer B at a flow rate of 1 ml/min. Fractions, containing np-moesin (132–156 ml) or ⁵⁵⁸T-p-moesin (140–164 ml) were pooled, and NaCl was added to 1 M final concentration.

Phenyl-Sepharose Chromatography. Phenyl-Sepharose CL-4B column (15 \times 57 mm; Pharmacia) was washed with ethanol, followed by buffer B containing 1 M NaCl. After loading the sample from step 2, the column was washed with 100 ml of buffer A at 1 ml/min. Moesin was eluted with buffer A containing 1% Triton X-100. Fractions containing moesin (20–28 ml) were pooled.

Diethylaminoethyl (DEAE) Cellulose Chromatography. The pooled fractions from step 4 were loaded onto a DEAE-cellulose column (15 \times 57 mm, Whatman, Maidstone, England; DE52), equilibrated with 5 mM Tris-HCl, pH 7.5, 0.01% sodium azide. Moesin was eluted with a linear salt gradient (200 ml) from 0 to 400 mM KCl in the equilibrating buffer at a flow rate of 1 ml/min. Fractions containing moesin (30–42 ml) were pooled and dialyzed against buffer M (5 mM Tris-HCl, pH 7.5, 150 mM KCl, 0.01% sodium azide).

When other proteins, especially actin, contaminated the preparations, further purification was performed by gel filtration chromatography on Superose 12HR10/30 (10 \times 300 mm; Pharmacia) equilibrated with 10 mM Tris-HCl, pH 7.5, 150 mM NaCl, 0.005% Triton X-100. This step was usually needed, particularly when columns in steps 1–4 had been reused. The highly purified preparations were finally stored at 4°C.

Purification of Actin Isoforms

α -Actin was prepared from rabbit skeletal muscle with some modifications of a previously published procedure (Spudich and Watt, 1971). Actin was extracted from acetone powder in buffer G (2 mM Tris-HCl, 0.2 mM CaCl₂, 0.2 mM DTT, 0.2 mM ATP, 0.005% sodium azide) and cycled through one round of polymerization. After centrifugation at $100,000 \times g$, F-actin was resuspended in buffer G and rechromatographed on Superdex 200pg (1.6 \times 600 mm; Pharmacia).

Platelet actin was prepared as previously described (Gordon *et al.*, 1977). DEAE-cellulose (Whatman, DE52), 200 ml (wet volume), was washed with 1 N HCl, 1 N NaOH, and water (2000 ml each) and then suspended in ~200 ml of buffer C (10 mM Tris-HCl, 0.2 mM Na₂ATP, 0.2 mM CaCl₂, 0.5 mM DTT, 0.005% sodium azide) containing 100 mM KCl. ATP (1.2 g) was added, and the pH was

readjusted to 7.5 with KOH. After 15 min the ATP-saturated DEAE-cellulose was packed into a column (2.5 \times 30 cm) and equilibrated with 400 ml of 100 mM KCl in buffer C. Washed human platelets (2×10^{11}) were homogenized in 20 ml of buffer G and centrifuged for 90 min at $100,000 \times g$ at 4°C. The extract was chromatographed on the DEAE-cellulose column. Forty milliliters of buffer G were applied immediately before and after the sample. The column was then eluted with 200 ml of 100 mM KCl in buffer C and 2 l of a linear gradient from 100 to 500 mM KCl in buffer C at 1 ml/min. Actin eluted between 190 and 240 mM KCl. Two-micromolar MgCl₂ was added, and the solution was warmed to 25°C for 60 min to polymerize actin. After centrifugation at $100,000 \times g$ for 3 h at 20°C, the pellet was homogenized in 20 ml of buffer G. The suspension was then dialyzed against three changes of buffer G for 60 h. Residual material was removed by centrifugation at $100,000 \times g$ for 90 min, and the depolymerized actin was applied to Superdex 200pg and eluted with buffer G. Actin-containing fractions were pooled in buffer G containing 2 mM MgCl₂ and 100 mM KCl to polymerize actin. After pelleting at $100,000 \times g$, F-actin was resuspended in buffer G and rechromatographed on Superdex 200pg.

F-Actin Overlay Assay

Platelets were lysed by addition of an equal volume of 2 \times SDS sample buffer at 70°C for 5 min. The samples were resolved by SDS-PAGE on a 9%, 0.75-mm-thick polyacrylamide gel run under reducing conditions at constant 120 V for 100 min at 20–25°C. The proteins were electrotransferred to nitrocellulose membranes (BA-85, 0.45 μ m pore size; Schleicher & Schuell, Keene, NH) at constant 5 mA/cm² for 60 min at room temperature using a semidry blotting apparatus (KS-8460; Marysol, Tokyo, Japan). Nitrocellulose blots were incubated overnight at 4°C in TTBS (20 mM Tris-HCl, pH 7.6, 137 mM NaCl, 0.05% Tween 20) containing 0.01% sodium azide to renature proteins and were blocked in 5% milk in TTBS for either 1 h at room temperature or overnight at 4°C before shipment from Japan to the United States.

The blots were blocked a second time with 5% milk, 90 mM NaCl, 0.05% (vol/vol) Tween 20, 10 mM Tris-HCl, pH 7.5 (TBST) and probed with 50 μ g/ml gelsolin-capped, phalloidin-stabilized, ¹²⁵I-labeled F-actin in TBST (Chia *et al.*, 1991). The blot was washed four or five times (2 min/wash) with TBST, air dried, and exposed either at 21°C to a phosphorimager screen or at –80°C to film in the presence of an intensifying screen. Alternatively, the blots were probed with 20 μ g/ml phalloidin-stabilized [α -³²P]ATP, prepared as described by Mackay *et al.* (1997) and Huang *et al.* (1999).

F-Actin Co-Sedimentation Assay in the Presence of Liposomes

F-actin was incubated with or without ⁵⁵⁸T- or np-moesin in buffer F (5 mM Tris-HCl, pH 7.5, 0.5 mM Na₂ATP, 2 mM MgCl₂, 140 mM NaCl, 0.2 mM DTT, 0.2 mM CaCl₂, 0.005% sodium azide) with or without various liposomes for 1 h at 37°C. In some experiments, lysoPC or Triton X-100 was added to the reaction mixture during the incubation. The filaments were then sedimented by centrifugation at $100,000 \times g$ for 20 min at 37°C. Proteins in the supernatants and pellets were then solubilized in SDS gel sample buffer and subjected to SDS-PAGE. Polypeptides in the gel were visualized by Coomassie brilliant blue staining.

Gel Shift Assay by SDS-PAGE

Phosphorylated or nonphosphorylated moesin (0.5 μ g), or α -actin (0.5 μ g) was incubated with various lipid vesicles (prepared with or without sonication; final concentration, 0.02%, wt/vol) in buffer F (final volume, 10 μ l) for 1 h at 37°C. For this assay, lipids were solubilized in water. In some experiments, after incubation with lipids, detergents (0.1%, unless noted otherwise, or 1%, wt/vol) or phospholipid (0.02%, wt/vol) were added, and the incubation was

continued at 37°C for 10 or 60 min. The reaction mixtures were then mixed with an equal volume of 2× SDS sample buffer and either heated for 10 min at 95°C or immediately loaded onto a 9% polyacrylamide gel (1 mm thick) and electrophoresed under reducing conditions at constant 160 V for 70 min at room temperature in a Hoefer SE250 minigel apparatus. Polypeptides in the gel were visualized by silver staining.

Affinity Precipitation Assay with Biotinylated Synthetic Peptides

Two biotinylated peptides of the following sequences from the C-terminal domain of CD44 were synthesized, purified, and characterized by mass spectroscopy by the Protein Chemistry Facility at Tufts University: biotin, IAVNSRRRCGQKQKLVINS (CD44cyt); and biotin, IAVNSAARCGQKQKLVINS (CD44cytAA, mutated control). Each peptide (2.5 µg) was added in 50 µl of buffer F and incubated with 10 µl of streptavidin-agarose 1:1 slurry for 1 h. After two washes with buffer F, ⁵⁵⁸T-p- or np-moesin (0.5 µg each) was added and incubation was continued in the presence or absence of lipids (0.01%, wt/vol), with or without 0.1% (wt/vol) Triton X-100, for an additional 1 h. In some experiments, F-actin (2 mg) was added, and the mixture was incubated for 1 h. All incubations were performed at 37°C. The beads were pelleted, and supernatants were removed. Bound proteins were eluted from the beads by boiling in SDS sample buffer and analyzed on 9% silver-stained SDS-PAGE gels.

F-Actin Co-Sedimentation Assay in the Presence of Detergents

F-actin was incubated for 1 h at 25°C with (or without) ⁵⁵⁸T-p- or np-moesin in buffer F and with or without various detergents. For some experiments, F-actin was incubated with phalloidin at molar ratios (actin/phalloidin) from 0.5 to 5 for 30 min at 25°C before addition of detergent and moesin. The filaments were then sedimented by centrifugation at 100,000 × g for 20 min at 25°C. Proteins in the supernatants and pellets were solubilized in SDS gel sample buffer and analyzed after SDS-PAGE and silver staining.

To determine the stoichiometry of moesin/F-actin binding, F-actin was incubated with phalloidin at a 1:2 (actin/phalloidin) molar ratio for 30 min at 25°C before addition of detergents with (or without) ⁵⁵⁸T-p- or np-moesin in buffer FK (5 mM Tris-HCl, pH 7.5, 0.5 mM Na₂ATP, 2 mM MgCl₂, 140 mM KCl, 0.2 mM DTT, 0.2 mM CaCl₂, 0.005% sodium azide). Incubations were continued for 1 h at 25°C. The actin filaments were sedimented by centrifugation at 100,000 × g for 20 min at 25°C. Proteins in the supernatants were precipitated with trichloroacetic acid containing 2 mg/ml sodium deoxycholate, and the precipitates were washed with ice-cold acetone, dissolved in SDS sample buffer, separated by SDS-PAGE, and analyzed by Coomassie blue staining or by immunoblotting with affinity-purified pAbMo or pAbKYKpTLR.

Isolation of DOTMAC- and Triton X-100-Insoluble Fractions

Platelets were lysed by adding an equal volume of 2× dodecyltrimethylammonium chloride (DOTMAC; Nacalai Tesque, Kyoto, Japan) lysis buffer (2% DOTMAC, 50 mM Tris-HCl, 10 mM EGTA, 100 mM NaCl, 2 mM MgCl₂, protease inhibitor mixture [20 µg/ml aprotinin, 20 µM E-64, 200 µM leupeptin, 200 µM p-amidinophenylmethanesulfonyl fluoride], 1 µM calyculin A, 5 mM sodium pyrophosphate, 1 µM staurosporine, 100 µM pervanadate, 10 µM phalloidin, 10 µg/ml Taxol). After 5 min on ice, the lysates were centrifuged at 15,600 × g for 4 min at 4°C. The resulting pellet (15K pellet) was solubilized in 1× SDS sample buffer. The 15K supernatant was centrifuged again at 100,000 × g for 30 min at 4°C, and proteins in pellets (100K pellet) and supernatants were solubilized with SDS sample buffer. For the Triton X-100 fractionation, 2% of

Triton X-100 was used instead of DOTMAC, and all other procedures were essentially identical. All samples were heated at 95°C, sonicated, and resolved by SDS-PAGE on a 10% polyacrylamide gel electrophoresed under reducing conditions as described (Nakamura *et al.*, 1995). Moesin, phosphorylated moesin, and actin were detected by immunoblotting and the enhanced chemiluminescence detection system.

Quantitation of Moesin

Amounts of ⁵⁵⁸T-p- and np-moesin were determined from the intensity of the bands on immunoblots developed with the antibodies described above using scanning densitometry and known amounts of recombinantly prepared moesin as the standard. Quantification was performed on blots prepared in parallel to blots used for F-actin binding experiments.

RESULTS

Phosphorylation of Moesin in Human Platelets

Stimulation of human platelets with thrombin is accompanied by a transient incorporation of ³²P_i into moesin at a single amino acid residue, ⁵⁵⁸threonine (Nakamura *et al.*, 1995). Subsequent to the initial observation, we prepared phosphorylation state-specific antibodies to both phosphorylated and nonphosphorylated synthetic peptides containing ⁵⁵⁸T (Nakamura *et al.*, 1996). The antibodies to the phosphorylated form of the peptide were more useful because of higher titers and greater specificity. This reagent (pAbKYKpTLR) reacted only with phosphorylated moesin, either immunoprecipitated from lysates of untreated platelets or platelets treated with calyculin A (Figure 1). The antibody was essentially unreactive with nonphosphorylated moesin isolated from staurosporine-treated platelets and also failed to react with any other protein in whole platelet lysates. Thus, the epitope recognized by this antibody is not shared by any other platelet protein. Consistent with the time course of phosphorylation established earlier using ³²P_i incorporation into moesin is the Western blot analysis of platelet lysates shown in Figure 1B. Given equivalent loading of lysates for each time point and assuming 100% phosphorylation of moesin in calyculin A-treated platelets (Nakamura *et al.*, 1995), the percentage of phosphorylated moesin molecules was calculated from the relative intensity of the moesin signal observed with pAbKYKpTLR. In resting platelets, ~25% of the moesin molecules were phosphorylated. This number varied somewhat depending on individual platelet preparations but was not significantly influenced by platelet storage. Although many of the experiments were performed with platelets isolated from outdated platelet-rich plasma, similar data were obtained with freshly prepared platelets. Within seconds after exposure to thrombin, a 1.3-fold increase to ~35% in the number of ⁵⁵⁸T-p-moesin molecules was observed, and this number decreased to ~15% within 1–2 min.

Platelets are quite sensitive to a variety of drugs. For instance, the phorbol ester PMA, the calcium ionophore A23187, and prostaglandin PGE₁ have been used extensively to study the mechanism of platelet activation. PMA and calcium ionophore A23187 activate protein kinase C (Kaibuchi *et al.*, 1983; Sano *et al.*, 1983); both treatments caused a transient increase in moesin phosphorylation (data not shown). On the other hand, PGE₁, which elevates cAMP

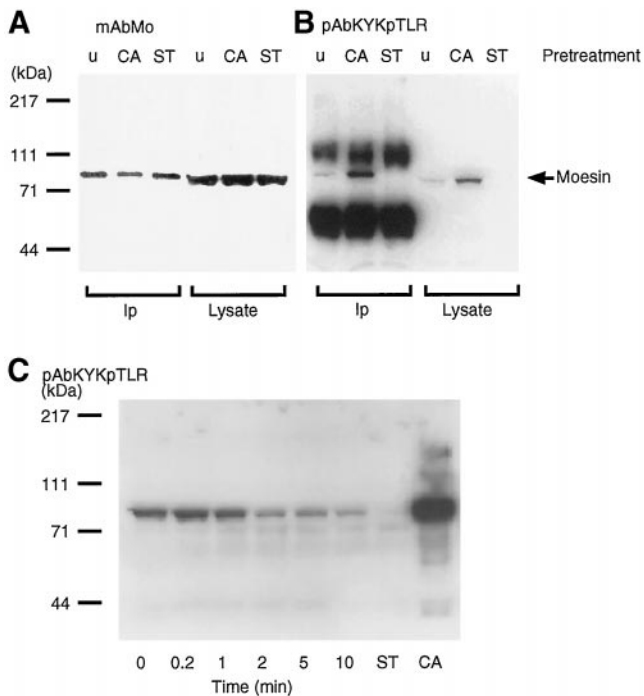


Figure 1. Detection and quantification of moesin phosphorylation at a single site, 558 threonine, in platelets by immunoblot analysis. (A) Immunoblot analysis with mouse monoclonal antibody (mAbMo) 38/87 of moesin immunoprecipitated with a polyclonal affinity purified anti-moesin reagent (pAbMo) from detergent extracts (Ip) and total platelet lysates: untreated (u), 100 nM calyculin A (CA), or 1 μ M staurosporine (ST) pretreated for 10 min. (B) Immunoblot analysis with rabbit polyclonal anti- 558 T-p-moesin raised to the peptide (pAbKYKpTLR) of the same samples as in A. The position of moesin is indicated with an arrow. The amounts of moesin in each of the three lanes of Ip and lysates are approximately the same (A). Note in B the increase in phosphorylation in the CA samples and the absence of a phosphorylated band in the ST samples in comparison with untreated platelets. The two dense bands in the Ip lanes of B are heavy- and light-chain polypeptides of rabbit IgG in the immunoprecipitate. (C) Immunoblot analysis of moesin phosphorylation in response to thrombin stimulation of platelets. Aliquots of total platelet lysates were electrophoresed on 9% SDS-polyacrylamide gels and blotted after protein transfer to nitrocellulose with pAbKYKpTLR antibodies as in B. ST and CA refer to lysates from platelets pre-treated with staurosporine or calyculin A as in A. Molecular mass standards are shown on the left. The blot is representative of three separate experiments.

levels in the cytosol and inhibits platelet activation, led to rapid dephosphorylation of moesin within 1 min. These results suggest that phosphorylation of moesin correlates with the state of platelet activation, which may be influenced by different kinases and phosphatases depending on the nature of the stimulus.

Isolation of Phosphorylated and Nonphosphorylated Moesin from Human Platelets

When stimulated with thrombin or when exposed to a surface such as glass, platelets change shape by spreading and by protruding filopodia, characteristic extensions of the

plasma membrane that contain moesin and actin filaments (Nakamura *et al.*, 1995). To address the relationship between phosphorylation of moesin and binding to actin filaments more directly, np- and 558 T-p-moesin were purified from human platelets that had been pretreated with staurosporine or calyculin A, respectively. Figure 2A shows the first purification step on heparin-agarose for moesin from platelets treated with 100 nM calyculin A for 30 s. These conditions induced phosphorylation of \sim 50% of total moesin as confirmed by immunoblotting (our unpublished data). Moesin eluted in two major peaks at 190–220 mM NaCl and 260–290 mM NaCl, respectively (Figure 2B). Monoclonal anti-moesin and pAbKYKTLR antibodies reacted with both forms of moesin (Figure 2B). When lysates of staurosporine-treated platelets were analyzed, the second peak was completely eliminated (our unpublished data), and this peak became the major peak in calyculin A-treated platelets. The first peak contains only np-moesin, and the second contains exclusively 558 T-p-moesin, as confirmed with the pAbKYKpTLR antibody reagent (Figure 2, B–D). The purification scheme for 558 T-p- and np-moesin included sequential chromatography on columns of blue Sepharose, phenyl-Sepharose, and DEAE-cellulose ion exchange chromatography (details in MATERIALS AND METHODS). 558 T-p-moesin was considerably enriched after the blue- and phenyl-Sepharose steps and was a single Coomassie blue-stained band after final purification on DEAE-cellulose (Figure 2E). Similar data were obtained for np-moesin, and the final purified preparations proved to be homogeneous by silver staining (our unpublished results) and two-dimensional electrophoresis (Figure 2F). No differences in properties were seen by gel permeation chromatography or sucrose gradient centrifugation in 0.1% Triton X-100 or 0.1% DOTMAC. Both forms of moesin appeared to be monomeric, indicating that no detectable changes in moesin association state accompanied phosphorylation.

Phosphorylated Moesin Binds Actin Filaments by Blot Overlay

Using the two highly purified and well-characterized forms of platelet moesin, we asked whether phosphorylation of 558 threonine affects moesin binding to rabbit skeletal muscle α - and β/γ -actin from platelets *in vitro*. β -Actin was chosen because this isoform is localized in subcortical regions of cells and because a preference for this isoform was reported in experiments with ezrin isolated from gastric parietal cells.

As shown in Figure 3A, F-actin bound weakly on blot overlays to purified platelet np-moesin and strongly to 558 T-p-moesin. F-actin binding of moesin was also increased in platelets that had been activated with thrombin or pretreated with calyculin A; increased F-actin binding correlated well with the increased amounts of 558 T-p-moesin molecules (Figure 3B). Whether labeled directly with the 125 I-Bolton-Hunter method (Figure 3B) or indirectly by incorporation of [32 P]ATP during polymerization (Figure 3C), the F-actin probe usually bound weakly to recombinant moesin and to moesin from staurosporine-treated platelets. Increases and decreases in F-actin binding on overlays closely followed the kinetic response of moesin phosphorylation upon thrombin stimulation (our unpublished results).

Resting platelets and platelets treated with staurosporine gave somewhat variable results. Although in some experiments a signal was not detectable in staurosporine-treated

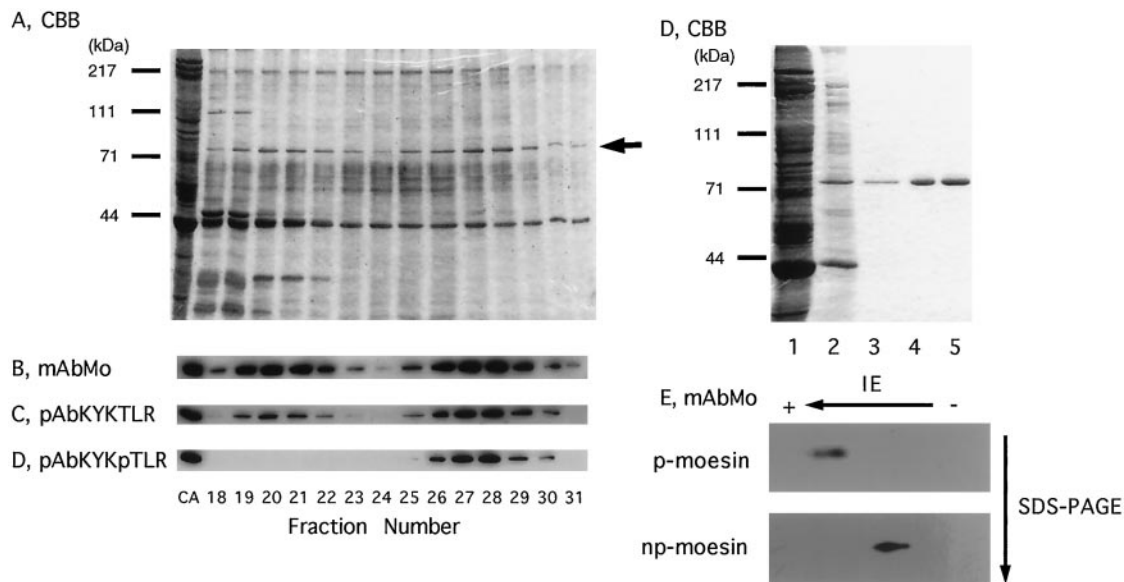


Figure 2. Purification of ^{558}T -phosphorylated and unphosphorylated moesin from human platelets. Human platelets were treated with 100 nM calyculin A for 30 s at 37°C , which produces $\sim 50\%$ of phosphorylated moesin (p-moesin). A cell lysate was prepared as described in MATERIALS AND METHODS and loaded onto a heparin-agarose column (15×57 mm). Proteins were eluted with a 200-ml linear gradient of 0–500 mM NaCl in equilibrating buffer at a flow rate of 1 ml/min, and fractions of 4 ml were collected and analysed by SDS-PAGE (A; CBB, Coomassie brilliant blue–stained gel) and immunoblot analysis (B–D). Analysis of fraction numbers 18–31 is shown, and a lysate of calyculin A-treated platelets served as the positive control in lane 1 (CA). Blots were developed with monoclonal moesin antibodies (B; mAbMo) and affinity-purified polyclonal moesin peptide (C; pAbKYKTLR) or moesin phosphopeptide antibodies (D; pAbKYKpTLR). The position of moesin is indicated by the arrow in A. In E, the Coomassie brilliant blue–stained gel shows the protein profile of fractions containing ^{558}T -p-moesin in the different chromatographic steps: lane 1, total platelet lysate; lane 2, ^{558}T -p-moesin eluted from heparin-agarose; lane 3, eluate from blue-Sepharose; lane 4, eluate from phenyl-Sepharose; and lane 5, final product after DEAE-cellulose. Molecular mass standards are shown in A and D. In F, immunoblots of purified ^{558}T -p-moesin and nonphosphorylated (np-) moesin after two-dimensional electrophoretic separation show homogeneous spots. The blots were developed with monoclonal antibodies to moesin (mAbMo).

platelet lysates (Figure 3C), in other experiments the signal was as strong as that shown in Figure 3B. Variations in protein amount can be excluded, because Western blotting with antibodies was used for every experiment, and there was no indication of protein loss during transfer. Detection of the F-actin binding activity of moesin in the blot overlay assay depends on protein concentration but could also be sensitive to factors that impact denaturation and renaturation of the protein on the nitrocellulose filter. This is the case under certain conditions, because precipitation with acetone considerably increased F-actin binding to nonphosphorylated moesin (our unpublished results). The example shown in Figure 3C is, however, entirely consistent with a rather close correlation between F-actin binding signal and the amount of ^{558}T -p-moesin but not the amount of total moesin. This result suggests that secondary structural elements that can regulate the moesin interaction with F-actin are normally retained, or regained, after SDS-PAGE and electrotransfer to nitrocellulose.

Co-Sedimentation of F-Actin and ^{558}T -p-Moesin in Cationic Detergents

We also examined the interaction between purified moesin and F-actin by co-sedimentation. Both forms of platelet moesin tended to aggregate, and $>60\%$ of each form sedimented,

even in the absence of F-actin. We screened a number of detergents, searching for conditions that maintained moesin in solution, had a negligible effect on actin filament stability, and facilitated moesin association with F-actin (Table 1). Although moesin solubility was achieved with a number of nonionic, anionic, or amphoteric detergents, both below and above their critical micelle concentration (Igarashi, 1987), we found that the best conditions for this assay included the cationic detergents cetyltrimethylammonium chloride or DOTMAC. In these detergents, ^{558}T -p-moesin pelleted specifically with F-actin (Figure 4). No interaction between F-actin and either form of moesin was observed in any concentration of Triton X-100 or other nonionic or amphoteric detergent (our unpublished results).

^{558}T -p-Moesin and F-actin Associate with High Affinity

In 0.1% DOTMAC, much more p-moesin than np-moesin co-sedimented with F-actin (Figure 4A). However, this concentration of DOTMAC had a slight effect on actin filaments, because the amount of actin remaining in the supernatant was increased relative to that observed in experiments performed in the absence of detergent (our unpublished results). When phalloidin was added at a 1:2 (actin:phalloidin) ratio, little or no actin remained in the high-speed superna-

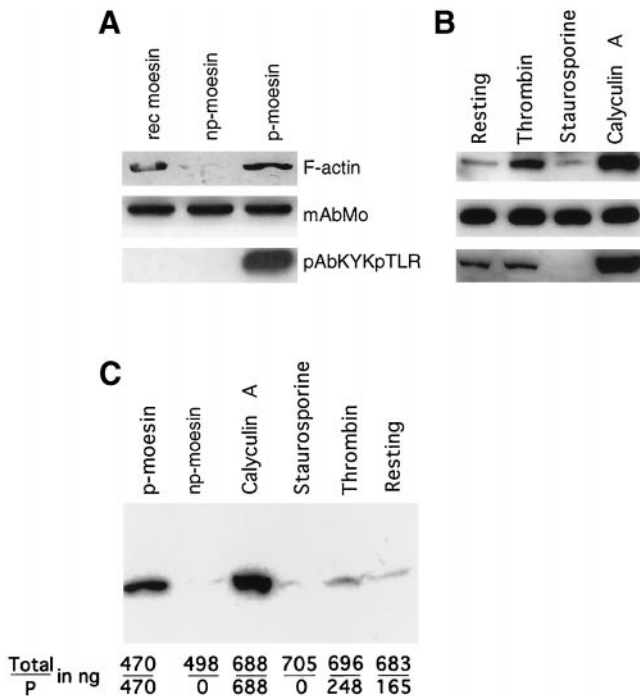


Figure 3. F-actin blot overlay detects binding to the phosphorylated form of moesin in platelet lysates and after purification. Proteins were separated by SDS-PAGE, transferred to nitrocellulose filters, and blotted with a ^{125}I -labeled F-actin probe in A and B and with a ^{32}P ATP-labeled probe in C. Before this analysis, the amounts of immunoreactive moesin were estimated by densitometric analysis and comparison with known amounts of recombinant moesin. The loaded amount of moesin is indicated in nanograms. (A) Binding of F-actin to purified recombinant moesin made in bacteria (470 ng; rec moesin, lane 1) and to purified phosphorylated platelet moesin (500 ng; p-moesin, lane 3). Nonphosphorylated moesin (498 ng; np-moesin, lane 2) does not bind appreciably to the probe. Parallel blots were processed with monoclonal moesin antibodies (mAbMo) or with antibodies specific for phosphorylated moesin (pAbKYKpTLR), indicating comparable protein loads and lack of detectable phosphorylation signals for rec moesin and np-moesin. (B) F-actin and antibody blots of total lysates of resting platelets (lane 1; 496 ng), platelets activated with thrombin for 10 s (lane 2; 502 ng), and platelets treated for 10 min with staurosporine (483 ng) or calyculin A (497 ng). Note the increase in F-actin signal intensity caused by thrombin stimulation in comparison with resting platelets and in relation to the maximal signal detected after calyculin A pretreatment. This relationship is also apparent from the immunoblot with phosphorylation-specific antibodies. (C) The amount of purified phosphorylated (p-) and nonphosphorylated (np-) moesin and of the two forms of moesin in platelet lysates of calyculin A-, staurosporine-, and thrombin-treated or resting platelets was quantified by immunoblotting and scanning densitometry as described in MATERIALS AND METHODS. The data shown represent total moesin and p-moesin in nanograms (total/P). Note again the absence of F-actin binding to platelet moesin in the absence of phosphorylation and increased binding signal resulting from the increase in phosphorylation caused by thrombin stimulation or by calyculin A.

tants, and the specificity of binding was maintained (Figure 4B). Essentially all of both the ^{558}T -p-moesin (0.5 μM) and the actin (5 μM) pelleted under these conditions. ^{558}T -p-moesin co-sedimented equally well with either rabbit skeletal α -actin or human platelet β,γ -actin (Figure 4C). Binding

in DOTMAC was specific for actin filaments, because neither purified ^{558}T -p-moesin nor np-moesin co-sedimented with Taxol-stabilized microtubules, which are also negatively charged biological polymers (our unpublished results). Binding in DOTMAC depended solely on the phosphorylation state of platelet moesin, independent of any other variable in the purification process, because removal of the phosphate from ^{558}T Thr by incubation with a purified platelet phosphatase eliminated binding to F-actin in this co-sedimentation assay (Hishiya and Nakamura, submitted for publication).

We further characterized the association between ^{558}T -p-moesin and F-actin by quantifying the amount of moesin that co-sedimented with increasing amounts of actin (0.5–5.0 μM) and by quantifying the amount of co-sedimented moesin when the ^{558}T -p-moesin concentration was varied from 1 to 5 μM (Figure 5, A and B). At physiological ionic strength, ^{558}T -p-moesin bound in a saturable manner to F-actin with a stoichiometry of 1:1, relative to monomeric actin (Figure 5C). Similar stoichiometries were observed with β,γ -actin (our unpublished results). From Scatchard analyses the dissociation constant (K_d) for the interaction between p-moesin and either actin isoform was ~ 10 nM. We next varied the concentration of phosphorylated moesin over the range of 1.5–30 nM, while keeping the actin concentration constant at 200 nM (Figure 5D). No free ^{558}T -p-moesin was detected in the supernatant even at the lowest p-moesin concentration (1.5 nM), suggesting that the K_d is < 1.5 nM. An accurate determination of affinities would require measurements to be made at protein concentrations at or below the value of K_d . This is not possible, because 0.5 nM is the detection limit in this assay system. A K_d on the order of 10^{-9} M is high compared with other actin-associated proteins (Gilmore and Burridge, 1996; Roy *et al.*, 1997) and suggests that the rate of p-moesin dissociation from F-actin is negligibly small under these conditions.

Finally, we investigated whether the association of ^{558}T -p-moesin is influenced by np-moesin. As shown in Figure 5E, ^{558}T -p-moesin selectively co-sediments with F-actin when both forms are mixed together at an equal ratio. This suggests that unmodified platelet moesin molecules neither associate with ^{558}T -p-moesin molecules nor interfere with the binding of ^{558}T -p-moesin to filamentous actin under these experimental conditions.

Association of Moesin with the DOTMAC-Insoluble Cytoskeleton is Contingent upon Phosphorylation of ^{558}T

Thrombin induces platelet aggregation (Schoenwaelder *et al.*, 1994) caused by increased cell-to-cell contacts that are mediated by integrins and adhesive proteins (Packham, 1994). This process is associated with a rapid redistribution of cytoskeletal proteins, as has been shown by the analysis of nonionic detergent lysates (Fox *et al.*, 1993). Most cytoplasmic actin filaments in platelets are recovered in the detergent-insoluble pellet after low-speed centrifugation, whereas membrane-bound F-actin filaments and membrane skeleton proteins, such as vinculin or talin, sediment at much higher speed (Fox, 1993).

The cytoskeletal association of ^{558}T -p-moesin was maintained after platelets were extracted with DOTMAC, but not

Table 1. Summary of the effect of detergents on stability of actin filaments, solubility of moesin, and association of moesin with F-actin in the co-sedimentation assay

| Detergents | cmc (%, wt/vol) ^a | Concentration tested (%, wt/vol) | F-actin in pellet (%) ^b | np-Moesin/p-moesin in pellet (%) ^b | np-Moesin/p-moesin in pellet with F-actin (%) ^b |
|------------------|---------------------------------|-------------------------------------|---------------------------------------|--|--|
| None | | | 93 | 60/62 | (55/62) |
| Nonionic | | | | | |
| Triton X-100 | 0.016 | 0.005 | 94 | 3/2 | (4/4) |
| | | 0.1 | 94 | 2/2 | (3/4) |
| Tween 20 | 0.006 | 0.001 | 93 | 0/0 | (0/0) |
| | | 0.1 | 86 | 0/0 | (0/0) |
| OG | 0.7 | 0.1 | 95 | 2/4 | (2/4) |
| | | 1.0 | 94 | 0/4 | (0/4) |
| DMDOAO | 0.048 | 0.01 | 95 | 0/0 | (0/0) |
| | | 0.1 | 96 | 0/0 | (0/0) |
| Amphoteric | | | | | |
| CHAPS | 0.5 | 0.1 | 70 | 0/0 | (0/0) |
| | | 1.0 | 45 | 0/0 | (0/0) |
| Anionic | | | | | |
| SDS | 0.24 | 0.05 | 0 | 0/0 | (0/0) |
| | | 1.0 | 0 | 0/0 | (0/0) |
| SDS ^c | 0.2 | 0.05 | 91 | 45/95 | (47/95) |
| | | 1.0 | 48 | 2/3 | (2/2) |
| Cationic | | | | | |
| CETMAC | 0.033 | 0.01 | 87 | 0/0 | (0/100) ^d |
| | | 0.1 | 14 | 0/0 | (0/5) |
| DOTMAC | 0.4 | 0.1 | 81 | 0/0 | (14/85) ^d |
| | | 1.0 | 8 | 0/0 | (0/2) |
| DOPC | 0.04 | 0.01 | 95 | 16/93 | (18/94) |
| | | 0.1 | 36 | 0/3 | (0/5) |

Phosphorylated (p-) or unphosphorylated (np-) moesin isolated from platelets was incubated with detergents in the presence or absence of actin filaments for 1 h at 37°C before centrifugation. Proteins of supernatant and pellet fractions were quantitated after SDS-PAGE and Coomassie brilliant blue staining by scanning densitometry. Percent indicates the amount of moesin in pellet fraction. OG, octyl- β -glucoside; DMDOAO, *N,N*-dimethyldodecylamine *N*-oxide; CHAPS, 3-[(cholamidylpropyl)-dimethyl ammonio]-1-propane sulfonate; CETMAC, cetyltrimethylammonium chloride; DOPC, dodecylpyridinium chloride.

^a Igarashi, 1987.

^b Data are presented as mean (n = 3), and each SD was <10% of the mean.

^c At pH 8.1

^d Significant difference between np-moesin and p-moesin by *t* test ($p < 0.001$).

with Triton X-100. When resting platelets were extracted with Triton X-100 (Figure 6A, left), ~80–95% of both total moesin and p-moesin were recovered in the 100K supernatant, and only small amounts remained associated with the cytoskeleton (~5% in the 15K pellet) and membrane skeleton (3.2% total moesin in the 100K pellet; Figure 6, B and C). In contrast, $53.4 \pm 4.2\%$ (mean \pm SD) of the actin sedimented in the Triton X-100-insoluble $15,600 \times g$ pellet of resting platelets. This amount increased and reached a peak of $78.4 \pm 2.4\%$ of the total platelet actin within 5 min after stimulation with thrombin (Figure 6D). This increase was accompanied by a corresponding loss of actin from the supernatant fraction (Figure 6D), consistent with an increased incorporation of actin into the cortical cytoskeleton. Because most of the $^{558}\text{T-p-moesin}$ was soluble even after calyculin A treatment, which results in essentially complete phosphorylation of moesin, phosphorylation alone is insufficient to retain moesin in the Triton X100-insoluble fraction.

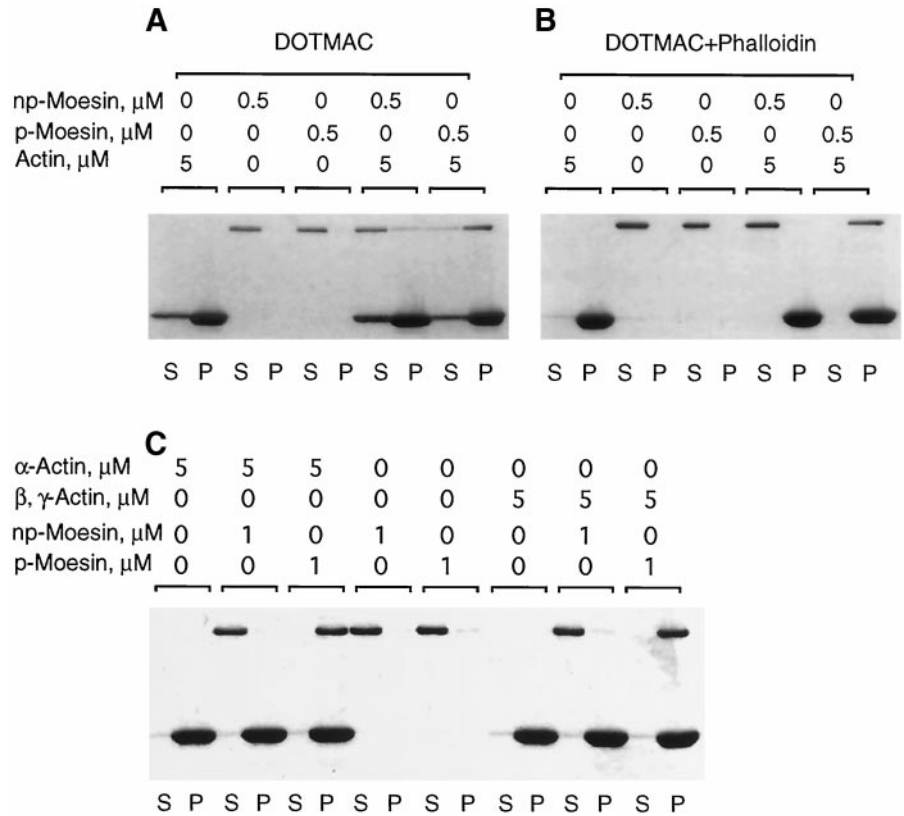
When platelets were fractionated with 1% DOTMAC (Figure 6, right), $^{558}\text{T-p-moesin}$ was quantitatively recovered with the

bulk of actin in the 15K cytoskeletal pellet (Figure 6F, right). The percentage of $^{558}\text{T-p-moesin}$ in this fraction also increased within seconds after thrombin stimulation (Figure 6F, right), with kinetics similar to that observed for moesin phosphorylation in total platelet lysates (Figure 1C). The amount of $^{558}\text{T-p-moesin}$ in the 15K pellet also increased after treatment with calyculin A (Figure 6F, right). By contrast, nearly all the np-moesin was recovered in the 100K soluble fraction (Figure 6E, right). Thus, the distributions of p-moesin and np-moesin in DOTMAC-fractionated platelets suggest that the association of moesin with the actin-based cytoskeleton *in vivo* is critically dependent on phosphorylation of ^{558}Thr in moesin, results consistent with our observations of phosphorylation-dependent binding to F-actin *in vitro*.

F-Actin Binding Site of $^{558}\text{T-p-Moesin}$ Exposed by Phosphatidylinositides

The requirement of a cationic detergent for binding of F-actin to moesin both *in vitro* and *in vivo* suggested that

Figure 4. Phosphorylated moesin selectively co-sediments with F-actin. (A) Purified phosphorylated (p-) or nonphosphorylated (np-) platelet moesin (0.5 μ M) was incubated either alone or together with rabbit skeletal α -F-actin (5 μ M) in DOTMAC-containing buffer for 1 h at 25°C before centrifugation, as described in MATERIALS AND METHODS. Equal volumes of supernatant (S) and pellet (P) fractions were analysed by SDS-PAGE, and proteins were visualized by Coomassie brilliant blue staining. The top band corresponds to moesin; the bottom band is actin. In the absence of actin, all of the moesin remains in the supernatant. Mixed with F-actin, a large fraction of p-moesin, but only a small fraction of np-moesin, co-sediments and appears in the pellet fraction. As can be seen, a fraction of actin remains in the supernatant, presumably because of a DOTMAC-induced increase in critical concentration for actin polymerization. When phalloidin is added to stabilize F-actin, essentially all of the actin is pelleted; p-moesin, but not np-moesin co-sediments with these phalloidin-stabilized filaments (B). (C) Under identical co-sedimentation conditions, p-moesin sediments equally well with skeletal muscle α - and platelet β , γ -actin.



phosphorylation was probably not the only contributing factor to the regulation and maintenance of moesin's F-actin-binding activity. Niggli *et al.* (1995), Hirao *et al.* (1996), and Huang *et al.* (1999) have shown that moesin-like proteins bind PI(4)P and PI(4,5)P₂. Because both cationic detergent and anionic lipids might act by disrupting potentially inhibitory electrostatic interaction(s), we examined the effects of charged phospholipids on the sedimentation behavior of the two forms of platelet moesin. Phospholipids at concentrations of 0.01% (wt/vol) in the form of multilamellar vesicles (L- α -phosphatidyl-L-serine, L- α -phosphatidylethanolamine, sphingomyelin, phosphatidylchlorine, phosphatidylglycerol, and phosphatidic acid), alone or in combination, either increased sedimentation of both forms of moesin (70–80% with phosphatidylglyceride, >90% with phosphatidic acid) or had no effect on aggregation or binding activity in that ~60% of both forms of moesin sedimented in both the presence and absence of F-actin. In the presence of phosphatidylinositides [PI(3)P:diC16:0, PI(4)P, PI(3,4)P₂, PI(4,5)P₂, and PI(3,4,5)P₃:diC16:0], added as micelles or incorporated into small unilamellar vesicles together with phosphatidylcholine, 100% of both forms of moesin sedimented with or without actin (our unpublished data), suggesting an association of moesin with the negatively charged phospholipids. By contrast, moesin in the absence of actin did not sediment, when stabilized with mixed micelles of charged phospholipids (PI, PI(4)P, and PI(4,5)P₂) and 0.1% Triton X-100 or 0.01% lysophosphatidylcholine (Table 2). When F-actin was added to moesin solubilized with Triton X-100 and either PI(4)P or PI(4,5)P₂ at a detergent:phospholipid ratio of 10:1, ~50% of ⁵⁵T-p-moesin

selectively and specifically co-sedimented with F-actin (Table 2 and Figure 7). No co-sedimentation with F-actin was observed when PI was substituted for phosphatidylinositide phosphates.

The binding of moesin to PI(4,5)P₂ was so tight that this complex resisted disruption by SDS. This change was apparent as a shift of moesin from its normal migration position to slower-migrating species revealed as a smear by silver staining of the gel (Figure 8A). These products accounted for the loss of moesin from the normal position of migration, because no material was detected that might have been trapped on top of the gel. This apparent loss or gel shift of 78-kDa protein on SDS gels was not as pronounced for mixtures of moesin with PI and PI(4)P (Figure 8B). Heating the PI(4,5)P₂-moesin mixture for 5–60 min neither increased nor decreased the loss seen with short incubation times (our unpublished results). A weak effect reaching statistical significance at 60 min was noted, however, when the mixture was heated in the presence of 0.1% Triton X-100 (our unpublished data), and 1% Triton X-100 or Tween 20 completely prevented this gel shift in the presence of phosphatidylinositol biphosphate (PIP₂) apparently because of disruption of the complex. Thus, gel shift analysis can be used to demonstrate a direct and specific interaction between moesin and PI(4,5)P₂, as had previously been reported for α -actinin (Fukami *et al.*, 1992).

DISCUSSION

Currently available evidence suggests that members of the moesin family of proteins interact specifically with actin

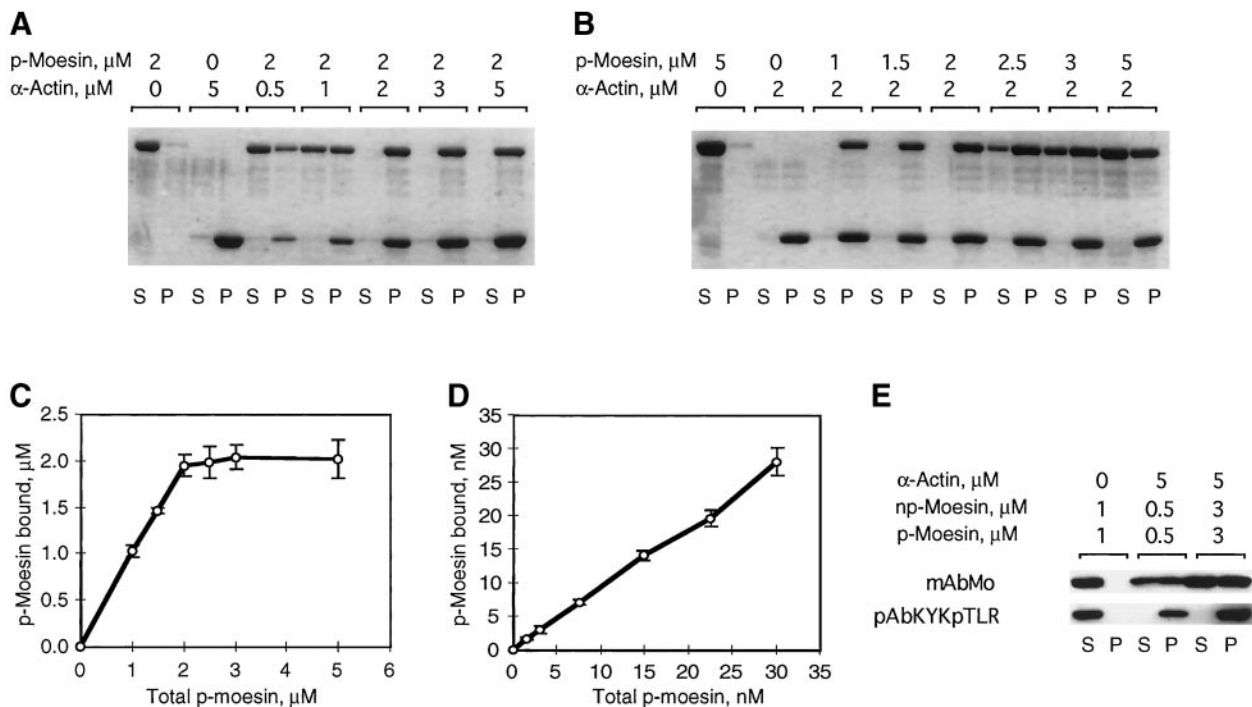


Figure 5. Phosphorylated moesin binds to filamentous actin with high affinity and at a ratio of 1:1. To define dissociation constants for the specific interaction between actin filaments and p-moesin in DOTMAC, co-sedimentation was done by keeping the p-moesin concentration fixed at 2 μM and varying the actin concentration from 0.5 to 5 μM (A) and by varying the p-moesin concentration from 1–5 μM at a fixed 2 μM concentration of actin (B). (C) Saturation binding analysis of p-moesin and α -actin at the micromolar level. Data were obtained under conditions described in B and are the mean \pm SD of three separate measurements. p-Moesin was varied over the range shown, whereas actin concentration was constant at 2 μM . (D) Binding analysis of p-moesin and α -actin at the nanomolar level. p-Moesin was varied over the range shown, whereas actin concentration was constant at 200 nM. Data are the mean \pm SD of three separate measurements derived from immunoblots probed with moesin antibodies. (E) Indicated amounts of p- and np-moesin were mixed before addition to actin filaments and centrifugation. The Western blot, developed with monoclonal antibodies to moesin (mAbMo) and p-moesin antibodies (pAbKYKpTLR), shows the distribution of the two moesin forms in supernatants (S) and pellets (P). Note that both forms remain in the supernatant in the absence of F-actin; all detectable p-moesin co-sediments with F-actin; increasing the amount of p- and np-moesin in the mixture yields expected amounts of p-moesin in the pellets, and np-moesin does not sediment as a mixed aggregate of p- and np-moesin.

filaments. This is most readily demonstrated with C-terminal fragments, which co-distribute with actin filaments and stress fibers in cells (Algrain *et al.*, 1993; Matsui *et al.*, 1998; Amieva *et al.*, 1999) and which bind directly to F-actin in solution binding assays (Turunen *et al.*, 1994; Pestonjamas *et al.*, 1995; Huang *et al.*, 1999). Detection of the F-actin binding activities of full-length, native proteins has been more difficult. This has not been directly demonstrated as yet *in vivo*, and several *in vitro* studies yielded remarkably discrepant results. Using co-sedimentation binding assays, Yao *et al.* (1996) determined a K_d of 50 nM, a stoichiometry of 1 ezrin bound for every 10 actin monomers, and isoform specificity for β -actin. This form of ezrin contains phosphoserine (Urushidani *et al.*, 1989; Hanzel *et al.*, 1991). Using bacterially expressed ezrin and a solid-phase assay, Roy *et al.* (1997) obtained a K_d of 504 ± 230 nM, a stoichiometry of 1 to 10.6 actin monomers, and approximately identical binding with filaments of α - or β / γ -actin. F-actin required both N- and C-terminal residues. A second site(s), which bound both F- and G-actin, was mapped between residues 288 and 333. By contrast, blot overlays and co-sedimentation assays with F-actin and *in vitro*-translated moesin indicated that only

the C-terminal domains of moesin, ezrin, and radixin interact with F-actin (Huang *et al.*, 1999); no binding to G-actin was observed (Pestonjamas *et al.*, 1995). Simons *et al.* (1998) phosphorylated a mixture of partially purified proteins *in vitro* at a ratio of 1 in 10 molecules presumably including threonine residues (Pietromonaco *et al.*, 1998). From their co-sedimentation data, Simons *et al.* (1998) calculated K_d values of 1.8 and 5 μM for moesin and ezrin, respectively, and found no isotype specificity.

Because of these discrepancies, we thought it important to isolate moesin from a cellular source. By taking advantage of previous work on platelets, we have been able to characterize two forms of moesin that differ only with respect to phosphorylation at a single residue (Nakamura *et al.*, 1995). This has made it possible to critically address the questions of whether and how the physiologically relevant phosphorylation at a conserved C-terminal residue, ⁵⁵⁸threonine, influences the F-actin binding potential of moesin and related proteins.

Our current interpretation of the cumulative data, including those presented here, is that the F-actin binding potential of full-length, cellular moesin *in vitro* is assay dependent

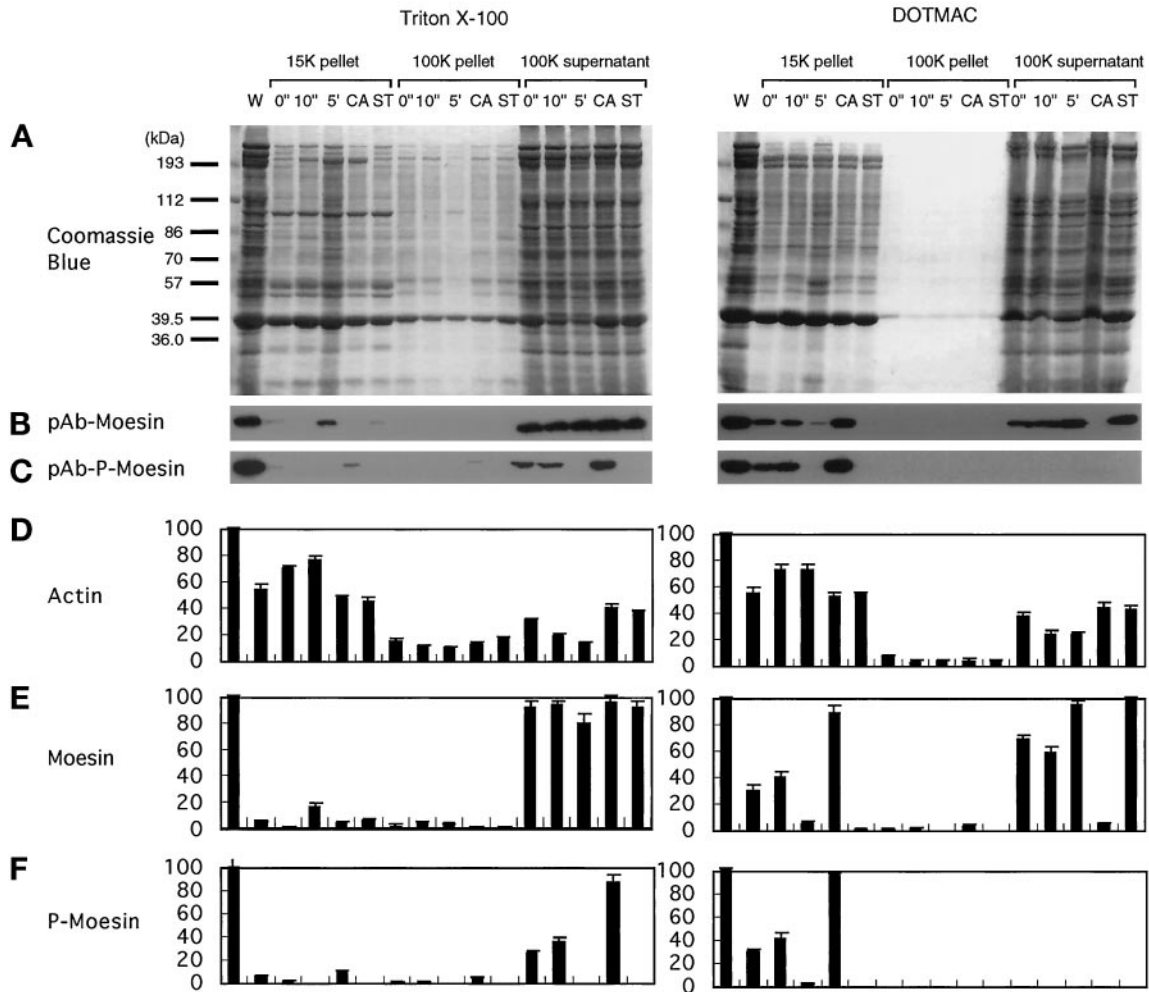


Figure 6. Phosphorylation-dependent association of moesin with the DOTMAC-insoluble cytoskeleton in thrombin-activated platelets. Platelets were lysed with Triton X-100 (left panels) or DOTMAC (right panels) lysis buffer at the indicated times (0 and 10 s and 5 min) after stimulation with 1 NIH unit/ml human thrombin at 37°C. Platelets were also incubated with 100 nM calyculin A (CA) or 1 μM staurosporine (ST) for 10 min before thrombin activation for 10 min. Lysates were centrifuged for 4 min at 15,600 × g, and the first supernatants were centrifuged for a further 30 min at 100,000 × g. Low- and high-speed pellets and high-speed supernatants were solubilized in SDS sample buffer, and the proteins were resolved by SDS-PAGE on a 9% gel and transferred to nitrocellulose membranes. (A) Coomassie brilliant blue-stained gels of the Triton X-100 (left) and DOTMAC (right) extraction and fractionation. After transfer of the proteins to nitrocellulose, blots were incubated with polyclonal antibodies to moesin (pAb-moesin; B) or phosphorylated moesin (pAb-p-moesin; C). Relative amounts of actin (D), moesin (E), and phosphorylated moesin (F) were obtained by densitometric analysis of the gels shown in A and the corresponding immunoblots of B and C. The blots shown in B and C are representative of three separate experiments. The data presented in D–E represent the means ± SD of three separate measurements. For detailed description and explanation, see text.

and that phosphorylation of ⁵⁵⁸threonine is one critical requirement. The blot overlay assay clearly distinguishes between phosphorylated and nonphosphorylated platelet moesin, with F-actin binding preferentially to phosphorylated platelet moesin. However, moesin made in bacteria also binds radiolabeled actin despite the fact that it is not phosphorylated. We have quantified this interaction by assuming that all p-moesin molecules measured with phosphorylation state-specific antibodies bind F-actin, whereas np-moesin does not. The data suggest that ~30% of recombinant moesin reacts with the F-actin probe. Experimentally, we can show that treating moesin with acetone effectively

converts platelet np-moesin to an F-actin binding form and enhances binding of the recombinant moesin. Similarly, boiling of cellular moesin, ezrin, or radixin in gel sample buffer containing SDS and dithiothreitol enhances their subsequent ability to bind F-actin in blot overlay assays. Furthermore, the isolated C-terminal domain binds actin constitutively, and phosphorylation or substitution of ⁵⁵⁸threonine does not change this activity (Matsui *et al.*, 1998; Huang *et al.*, 1999). These observations suggest that factors in addition to phosphorylation influence binding to the full-length proteins in this assay. The best explanation is incomplete or different folding during biosynthesis and/or analysis of the recombi-

Table 2. Summary of the effect of detergents, lipids, or detergent-mixed micelles on solubility of moesin and association of moesin with F-actin in the co-sedimentation assay

| Lipids | Concentration tested (%, wt/vol) | np-Moesin/p-moesin in pellet (%) ^a | np-Moesin/p-moesin in pellet with F-actin (%) |
|--------------------------------------|-------------------------------------|--|--|
| None | | 60/62 | (55/62) |
| Triton X-100 | | 2/2 | (3/4) |
| Triton X-100 + PI | 0.1/0.01 | 3/3 | (4/5) |
| Triton X-100 + PI(4)P | 0.1/0.01 | 3/4 | (5/47) ^{ab} |
| Triton X-100 + PI(4,5)P ₂ | 0.1/0.01 | 5/8 | (7/45) ^{ab} |
| LysoPC | 0.01 | 0/0 | (3/4) |
| LysoPC + PI | 0.01/0.01 | 2/3 | (5/4) |
| LysoPC + PI(4,5)P ₂ | 0.01/0.01 | 5/5 | (7/22) ^{**b} |

Phosphorylated (p-) or non-phosphorylated (np-) moesin isolated from platelets was incubated with detergents or detergent-mixed micelles in the presence or absence of actin filaments for 1 h at 37°C before centrifugation. Proteins in supernatants and pellets were quantitated after SDS-PAGE and Coomassie brilliant blue staining by scanning densitometry. Percent indicates the amount of moesin in pellet fraction. F-actin was stable in all conditions.

^a Data are presented as mean (n = 3) and each SD was <10% of the mean.

^b Significant difference between np-moesin and p-moesin by *t* test (* *p* < 0.001; ** *p* < 0.01).

nant and partial denaturation of mammalian proteins by SDS or acetone.

We found that small amounts of detergents are needed to prevent moesin from aggregating in solution and to permit the study of the interaction of purified platelet moesin with actin filaments by co-sedimentation binding assays. Minimization of aggregation and maintenance of F-actin binding are experimentally separable in that many detergents apparently stabilize moesin against aggregation without supporting binding to F-actin. Co-sedimentation of moesin with F-actin in solution binding assays apparently requires both phosphorylation of ⁵⁵⁸threonine and the presence of highly charged lipids. Both the cationic detergent DOTMAC and phosphatidylinositides support the binding of p-moesin, but not np-moesin, to actin filaments. Phosphorylation is critical because the quantifiable removal of the phosphate group by

a purified platelet phosphatase renders moesin inactive. Concentrations of DOTMAC that stabilize moesin against aggregation and also support phosphorylation-dependent binding to F-actin induce bundling of actin filaments, when analyzed by negative-staining electron microscopy (our unpublished results). Actin filament stability is not affected, except at much higher concentrations of DOTMAC. Because DOTMAC-solubilized np-moesin does not bind to actin filaments, DOTMAC apparently does not simply expose the F-actin binding site by denaturation, as we are proposing happens with acetone-mediated denaturation. Although the length of the hydrocarbon chains influences the effective concentration at which this detergent is active, its primary effect is probably through an interaction of the positively charged detergent head group with one or more of the highly conserved clusters of negatively charged amino acid

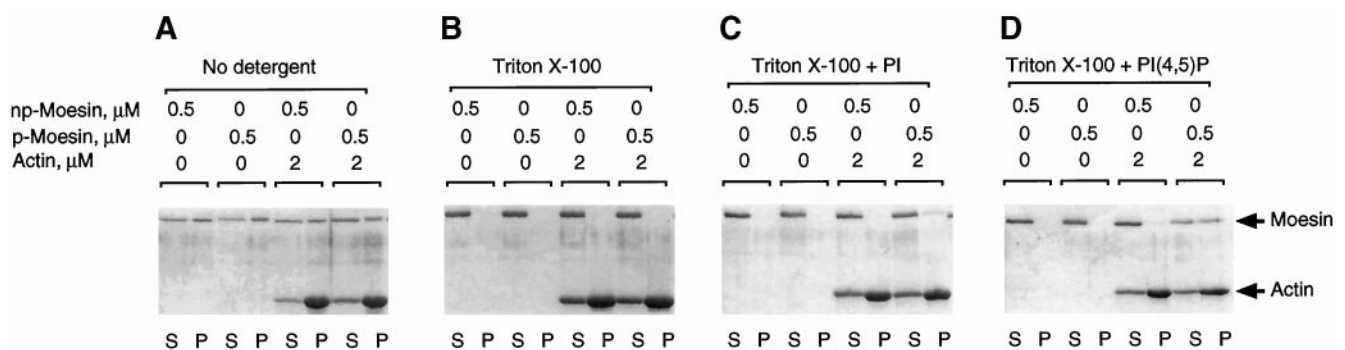


Figure 7. Phosphatidylinositol 4,5-bisphosphate is required for F-actin binding of phosphorylated moesin in Triton X-100. Phosphorylated (p-) and non-phosphorylated (np-) moesin isolated from platelets was incubated alone or in the presence of α -actin for 1 h at 37°C before sedimentation. In A, no detergent was added, and sizable fractions (~60%) of p- and np-moesin sedimented and were recovered in the pellet together with actin. There was no apparent difference between the two forms of moesin. In B, 0.1% Triton X-100 was added to the reaction mixtures. Both forms of moesin were soluble and did not sediment under this condition. In C and D, mixed micelles of 0.1% Triton X-100 and 0.01% phosphatidylinositol (PI) or phosphatidylinositol 4,5-bisphosphate (PIP₂) were added to the reaction mixtures. Approximately 50% of the total p-moesin co-sedimented together with actin in the presence of PIP₂. In all experiments, equal volumes of supernatant (S) and pellet (P) fractions were analysed by SDS-PAGE and Coomassie blue staining.

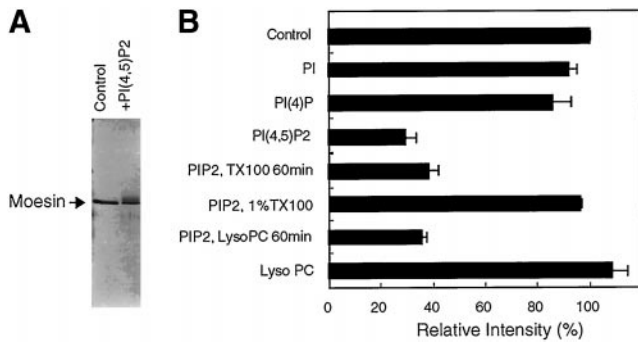


Figure 8. Gel shift induced by binding of phosphatidylinositol 4,5-bisphosphate to moesin on SDS polyacrylamide gels. Phosphorylated or nonphosphorylated moesin ($0.5 \mu\text{g}$) was incubated with sonicated PI, PI(4), PI(4,5)P₂, or LysoPC (lysophosphatidylcholine) in $10 \mu\text{l}$ of buffer F (final concentration, 0.02%, wt/vol) for 1 h at 37°C . In some experiments, 0.1% Triton X-100 or LysoPC was added, and the incubation was continued for an additional 1 h. The solutions were then solubilized with an equal volume of $2\times$ SDS sample buffer and run on a 9% polyacrylamide gel under reducing conditions. Proteins were stained with the silver method. (A) An example is shown for moesin and PI(4,5)P₂. Note the lower intensity of the band in the normal migration position. (B) The reduction in moesin under various conditions has been quantified by densitometry. The graph shows this loss as an indication of the gel shift that occurred in the presence of PI(4,5)P₂. This shift in migration is weakly influenced by a 60-min incubation in 0.1% Triton X-100 or LysoPC but is completely reversed in 1% Triton X-100.

residues in moesin (Lankes *et al.*, 1993). The binding constant between F-actin and moesin in DOTMAC is high in comparison with other actin-binding proteins, and we estimated the stoichiometry to be 1 moesin bound to 1 actin monomer. The magnitude of these values may be influenced by the bundling effect of DOTMAC on actin filaments.

We suggest that PI(4)P and PI(4,5)P₂ promote selective F-actin binding to p-moesin by binding tightly to moesin, because both p- and np-moesin are stabilized against aggregation or complex formation by these lipids below threshold concentrations (our unpublished results). Although binding constants for the interactions of polyphosphatidylinositides with moesin still need to be established, these negatively charged lipids are better candidates for physiological effectors than are positively charged lipids, which have not been reported in mammalian cells.

Polyphosphatidylinositides have been shown to regulate the activities of various other actin-binding proteins (Furuhashi *et al.*, 1992; Janmey, 1994) and to affect protein structure. For example, PIP₂ increases the α -helix content of profilin (Ragunathan *et al.*, 1992) and induces conformational changes of peptides (Lu and Chen, 1997). PIP₂ also dissociates the head-tail interaction of vinculin, unmasking its talin and actin binding sites (Gilmore and Burrige, 1996). Thus, binding of PIP₂ to sites on the N-terminal domain of moesin (Niggli *et al.*, 1995) could affect intramolecular structural features, as discussed below.

Mechanism of Activation of F-Actin Binding

The best explanation for the activation of F-actin binding of moesin is a conformational change caused by phosphoryla-

tion, cationic detergents, and polyphosphatidylinositides. Previously published data suggest the existence of a binding interaction between N- and C-terminal regions of ezrin, radixin, and moesin in the full-length, undenatured protein. This interaction has been demonstrated by *in vitro* assays with bacterially expressed GST fusion peptides of ezrin and radixin (Gary and Bretscher, 1995; Magendantz *et al.*, 1995), and by the yeast two-hybrid method with tagged and untagged fragments of moesin (Huang *et al.*, 1999). Recent structural data derived for a co-crystal of N- and C-terminal domains of moesin also indicate that two of three subregions of the N-terminal domain contact the C-terminal domain (Pearson *et al.*, 1998). Phosphorylation of ⁵⁵⁸threonine in the C-terminal domain inhibits the interaction with the N-terminal domain (Matsui *et al.*, 1998). Substitution of ⁵⁵⁸threonine with aspartate has the same effect (Huang *et al.*, 1999), indicating that a single negative charge is sufficient to prevent interaction. Indirect evidence is also provided by the much stronger binding of p-moesin to heparin in comparison with np-moesin. This constituted the basis for the successful separation of the two forms of moesin (Figure 3). The behavior of p-moesin during isolation is consistent with the exposure of additional positively charged residues to heparin and a structural change that is certainly larger than one would have expected from the additional single negative charge in p-moesin. The implication of these results for the intact protein is that structural disruption directly exposes the region of moesin that contains the F-actin binding site. Although previously proposed (Gary and Bretscher, 1995; Bretscher, 1999), this mechanism has not been formally established for the intact protein. Our experiments with isolated cellular proteins *in vitro* are consistent with the proposed activation of F-actin by disruption of the interaction between the N- and C-terminal domains, but our data also point toward additional contributory factors.

Evidence for a relatively large change in conformation comes from model studies with moesin mutants translated *in vitro*. Gary and Bretscher (1995) have shown that N- and C-terminal domains of recombinant ezrin associate with full-length denatured ezrin *in vitro*. According to their hypothesis, this is explained by the exposure of nondenatured F-actin binding sites through denaturation of N-terminal inhibitory sequences. We have compared full-length wild-type, Thr⁵⁵⁸Asp and various deletion mutant moesins for binding to N- and C-terminal domain probes (Huang *et al.*, 1999). In several assays, the ability of the full-length mutant to bind an additional domain of moesin parallels its F-actin binding activity. Binding of a relatively large 30-kDa peptide to the full-length protein requires a rather dramatic change in structure. Furthermore, when present, PIP₂ inhibits the interaction of the C-terminal domain to the full-length Thr⁵⁵⁸Asp mutant. This suggests that PIP₂ acts cooperatively and in concert with phosphorylation to expose the F-actin binding site.

Role and Regulation of Moesin Phosphorylation in Cells

How does phosphorylation of moesin contribute to cellular events during platelet activation? Thrombin-induced platelet shape change and secretion parallel the rapid increase in phosphorylation of a number of proteins (Fox, 1993; Holmsen and Dangelmaier, 1989). The phosphorylation of these

proteins occurs in three temporal phases that can be experimentally distinguished (Ferrell and Martin, 1988). First, the early phosphorylation of proteins such as P-selectin (Crovell *et al.*, 1993), actin-binding protein (Carroll and Gerrard, 1982), myosin light chains (Fox and Phillips, 1982), and p60^{src} (Clark and Brugge, 1993) occurs by an integrin-independent mechanism. Fibrinogen, by binding to the integrin receptor $\alpha_{IIb}\beta_3$ (GPIIb/IIIa), initiates a second wave of phosphorylation, which is followed by a third wave of platelet aggregation-dependent phosphorylation of proteins such as FAK (Lipfert *et al.*, 1992). Kinetic data suggest that moesin is one of protein substrates in the first wave of phosphorylation.

In platelets, signaling occurs primarily through members of the seven transmembrane-heterotrimeric G protein-coupled family of receptors (Zhang *et al.*, 1993; Chong *et al.*, 1994; Benka *et al.*, 1995) and through adhesion receptors (Torti *et al.*, 1994). As an effector of heterotrimeric G proteins, Rho acts on several targets, including Rho-dependent kinases and phosphatases. Moesin may be one of the targets for these enzymes. Rho-dependent kinase, however, does not efficiently modify the full-length protein *in vitro*, although recombinant C-terminal sequences of radixin are readily phosphorylated by this enzyme (Matsui *et al.*, 1998). Rac, Cdc42, and Rho also regulate phosphatidylinositide metabolism (Chong *et al.*, 1994; Carpenter *et al.*, 1997), and PIP₂ and Rho-dependent signaling pathways have been implicated in the association of moesin to plasma membrane constituents (Hirao *et al.*, 1996).

Our new insights regarding the requirements for the interaction of moesin with F-actin provide an opportunity to reevaluate these data. The incomplete information currently available does not make it clear which interactions are regulated, when, where, and by whom. For example, does PIP₂ primarily regulate interactions with membrane proteins, does it primarily regulate F-actin binding, or both? We also do not yet know whether ⁵⁵⁸Thr phosphorylation is required to activate moesin before binding to membrane proteins. We could envision dual effects and mechanisms in which PIP₂, by stabilizing interactions with membrane proteins, also presents moesin in a favorable conformation to be acted on by phosphokinases (Figure 9). We have attempted to reconstitute such a system *in vitro* with purified np-moesin, cytoplasmic fragments of CD44 that are known to associate with recombinant moesin, and PIP₂ (Hirao *et al.*, 1996; Legg and Isacke, 1998). However, we were not able to demonstrate binding of the CD44 cytoplasmic domain to either form of platelet moesin. This failure may derive from structural differences between platelet and recombinant moesin, or it may be due to the requirement for other, as yet unidentified regulatory components. These experiments did reveal, however, that F-actin binding of np-moesin was not activated, emphasizing the important role of phosphorylation. The reported redistribution of receptors (Helander *et al.*, 1996; Serrador *et al.*, 1997), formation of cell surface microextensions (Lamb *et al.*, 1997; Shaw *et al.*, 1998), and cell-cell interactions (Crepaldi *et al.*, 1997) mediated by moesin, ezrin, and radixin may depend on the proposed multistep mechanism of activation (Figure 9). Regulated binding to F-actin may serve to recruit receptors into filopodia; to create tension in the case of receptors attached to extracellular ligands (Zhang *et al.*, 1997), to redistribute receptors via treadmilling

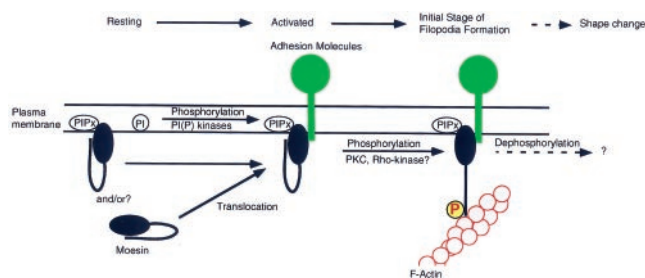


Figure 9. A multistep model for the regulation of the F-actin-binding activity of moesin in platelets. In the resting state, moesin is bound to as-yet-unknown membrane proteins or sites indicated by phosphatidylinositol polyphosphate (PIP_x). Membrane-bound moesin may exist in equilibrium with a soluble, cytosolic form. A first signal, perhaps involving PI(P) kinases, elevates levels of PIP₂. Moesin in a complex with other membrane components undergoes a conformational change, allowing it to become a substrate for a membrane-associated kinase, such as PKC or Rho-kinase. After phosphorylation at ⁵⁵⁸Thr, the F-actin binding function of moesin is activated, and linkage with actin filaments in the vicinity of the membrane may occur. Steady-state phosphorylation is maintained by the action of protein kinase(s) and protein phosphatase(s). Staurosporine and calyculin A shift the balance toward complete dephosphorylation or phosphorylation, respectively. Similarly, transient changes in the number of phosphorylated and activated moesin molecules, caused by an increase in kinase or a decrease in phosphatase activity, enhance the potential to form new membrane-cytoskeletal links.

of actin filaments or through the action of myosin motors (Mitchison and Kirschner, 1988), and/or to retrieve membrane during retraction of cell surface extensions (Amieva *et al.*, 1998). One could speculate that phosphorylation of residues other than ⁵⁵⁸Thr serves similar functions, but this needs to be evaluated (Krieg and Hunter, 1992; Fazioli *et al.*, 1993; Chen *et al.*, 1995). Our model allows recruitment to the membrane of moesin and other proteins to be regulated independently of F-actin attachment and provides a mechanism for ensuring tight spatial and temporal control of F-actin recruitment. It will be of some interest to test this model in cells, because changes at the membrane-cytoskeletal interface form an important part of cellular responses and may require more than one signal.

ACKNOWLEDGMENTS

We thank Dr. Katsuro Nishioka (Miyagi Red Cross Blood Center, Sendai, Japan) for providing platelets and S. Tsukita (Kyoto University) for purified recombinant mouse moesin from insect cells. These studies were supported in part by Nissan Science Foundation and a grant-in-aid for science research from the Ministry of Education, Science and Culture of Japan to F.N., who performed most of the work reported here. This research was also supported by grants from the Tobacco-related Research Program of the State of California, 4RT-0316, and US Public Health Service grants 1PO4-AR41045 to H.F. and GM-33048 to E.J.L.

REFERENCES

Algrain, M., Turunen, O., Vaheri, A., Louvard, D., and Arpin, M. (1993). Ezrin contains cytoskeleton and membrane binding domains

- accounting for its proposed role as a membrane-cytoskeletal linker. *J. Cell Biol.* 120, 129–139.
- Amieva, M.R., and Furthmayr, H. (1995). Subcellular localization of moesin in dynamic filopodia, retraction fibers, and other structures involved in substrate exploration, attachment, and cell-cell contacts. *Exp. Cell Res.* 219, 180–196.
- Amieva, M.R., Litman, P., Huang, L., Ichimaru, E., and Furthmayr, H. (1998). Disruption of dynamic cell surface architecture of NIH3T3 fibroblasts by the N-terminal domains of moesin and ezrin: in vivo imaging with GFP fusion proteins. *J. Cell Sci.* 112, 111–125.
- Benka, M.L., *et al.* (1995). The thrombin receptor in human platelets is coupled to a GTP binding protein of the G alpha q family. *FEBS Lett.* 363, 49–52.
- Bretscher, A. (1989). Rapid phosphorylation and reorganization of ezrin and spectrin accompany morphological changes induced in A431 cells by epidermal growth factor. *J. Cell Biol.* 108, 921–930.
- Bretscher, A. (1999). Regulation of cortical structure by the ezrin-radixin-moesin protein family. *Curr. Opin. Cell Biol.* 11, 109–116.
- Bretscher, A., Gary, R., and Berryman, M. (1995). Soluble ezrin purified from placenta exists as stable monomers and elongated dimers with masked C-terminal ezrin-radixin-moesin association domains. *Biochemistry* 34, 16830–16837.
- Carpenter, C.L., Toliás, K.F., Couvillon, A.C., and Hartwig, J.H. (1997). Signal transduction pathways involving the small G proteins rac and Cdc42 and phosphoinositide kinases. *Adv. Enzyme Regul.* 37, 377–390.
- Carroll, R.C., and Gerrard, J.M. (1982). Phosphorylation of platelet actin-binding protein during platelet activation. *Blood* 59, 466–471.
- Chen, J., Cohn, J.A., and Mandel, L.J. (1995). Dephosphorylation of ezrin as an early event in renal microvillar breakdown and anoxic injury. *Proc. Natl. Acad. Sci. USA* 92, 7495–7499.
- Chia, C.P., Hitt, A.L., and Luna, E.J. (1991). Direct binding of F-actin to ponticulín, an integral plasma membrane glycoprotein. *Cell Motil. Cytoskeleton* 18, 164–179.
- Chong, L.D., Traynor-Kaplan, A., Bokoch, G.M., and Schwartz, M.A. (1994). The small GTP-binding protein Rho regulates a phosphatidylinositol 4-phosphate 5-kinase in mammalian cells. *Cell* 79, 507–513.
- Clark, E.A., and Brugge, J.S. (1993). Redistribution of activated pp60c-src to integrin-dependent cytoskeletal complexes in thrombin-stimulated platelets. *Mol. Cell Biol.* 13, 1863–1871.
- Crepaldi, T., Gautreau, A., Comoglio, P.M., Louvard, D., and Arpin, M. (1997). Ezrin is an effector of hepatocyte growth factor-mediated migration and morphogenesis in epithelial cells. *J. Cell Biol.* 138, 423–434.
- Crovello, C.S., Furie, B.C., and Furie, B. (1993). Rapid phosphorylation and selective dephosphorylation of P-selectin accompanies platelet activation. *J. Biol. Chem.* 268, 14590–14593.
- Egerton, M., Burgess, W.H., Chen, D., Druker, B.J., Bretscher, A., and Samelson, L.E. (1992). Identification of ezrin as an 81-kDa tyrosine-phosphorylated protein in T cells. *J. Immunol.* 149, 1847–1852.
- Fallon, R.J. (1990). Staurosporine inhibits a tyrosine protein kinase in human hepatoma cell membranes. *Biochem. Biophys. Res. Commun.* 170, 1191–1196.
- Fazioli, F., Wong, W.T., Ullrich, S.J., Sakaguchi, K., Appella, E., and Di Fiore, P.P. (1993). The ezrin-like family of tyrosine kinase substrates: receptor-specific pattern of tyrosine phosphorylation and relationship to malignant transformation. *Oncogene* 8, 1335–1345.
- Ferrell, J.E., Jr., and Martin, G.S. (1988). Platelet tyrosine-specific protein phosphorylation is regulated by thrombin. *Mol. Cell Biol.* 8, 3603–3610.
- Fox, J.E. (1993). The platelet cytoskeleton. *Thromb. Haemost.* 70, 884–893.
- Fox, J.E., Lipfert, L., Clark, E.A., Reynolds, C.C., Austin, C.D., and Brugge, J.S. (1993). On the role of the platelet membrane skeleton in mediating signal transduction. Association of GP IIb-IIIa, pp60c-src, pp62c-yes, and the p21ras GTPase-activating protein with the membrane skeleton. *J. Biol. Chem.* 268, 25973–25984.
- Fox, J.E., and Phillips, D.R. (1982). Role of phosphorylation in mediating the association of myosin with the cytoskeletal structures of human platelets. *J. Biol. Chem.* 257, 4120–4126.
- Fukami, K., Furuhashi, K., Ingaki, M., Endo, T., Hatano, S., and Takenawa, T. (1992). Requirements of phosphatidylinositol 4,5-bisphosphate for alpha-actinin function [see comments]. *Nature* 359, 150–152.
- Funayama, N., Nagafuchi, A., Sato, N., Tsukita, S., and Tsukita, S. (1991). Radixin is a novel member of the band 4.1 family. *J. Cell Biol.* 115, 1039–1048.
- Furuhashi, K., Inagaki, M., Hatano, S., Fukami, K., and Takenawa, T. (1992). Inositol phospholipid-induced suppression of F-actin-gelating activity of smooth muscle filamin. *Biochem. Biophys. Res. Commun.* 184, 1261–1265.
- Gary, R., and Bretscher, A. (1995). Ezrin self-association involves binding of an N-terminal domain to a normally masked C-terminal domain that includes the F-actin binding site. *Mol. Biol. Cell* 6, 1061–1075.
- Gilmore, A.P., and Burridge, K. (1996). Regulation of vinculin binding to talin and actin by phosphatidylinositol-4-5-bisphosphate. *Nature* 38, 531–535.
- Gordon, D.J., Boyer, J.L., and Korn, E.D. (1977). Comparative biochemistry of non-muscle actins. *J. Biol. Chem.* 252, 8300–8309.
- Gould, K.L., Bretscher, A., Esch, F.S., and Hunter, T. (1989). cDNA cloning and sequencing of the protein-tyrosine kinase substrate, ezrin, reveals homology to band 4.1. *EMBO J.* 8, 4133–4142.
- Gould, K.L., Cooper, J.A., Bretscher, A., and Hunter, T. (1986). The protein-tyrosine kinase substrate, p81, is homologous to a chicken microvillar core protein. *J. Cell Biol.* 102, 660–669.
- Hanzel, D., Reggio, H., Bretscher, A., Forte, J.G., and Mangeat, P. (1991). The secretion-stimulated 80 k phosphoprotein of parietal cells is ezrin, and has properties of a membrane cytoskeletal linker in the induced apical microvilli. *EMBO J.* 10, 2363–2373.
- Hartwig, J.H., Bokoch, J.M., Carpenter, C.L., Janmey, P.A., Taylor, L.A., Toker, A., and Stossel, T.P. (1995). Thrombin receptor ligation and activated rac uncap actin filament barbed ends through PI synthesis in permeabilized human platelets. *Cell* 82, 643–653.
- Helander, T.S., Carpen, O., Turunen, O., Kovanen, P.E., Vaheri, A., and Timonen, T. (1997). Icam-2 redistributed by ezrin as a target for killer cells. *Nature* 382, 265–268.
- Hirao, M., Sato, N., Kondo, T., Yonemura, S., Monden, M., Sasaki, T., Takai, Y., Tsukita, S., and Tsukita, S. (1996). Regulation mechanism of ERM (ezrin/radixin/moesin) protein/plasma membrane association: possible involvement of phosphatidylinositol turnover and Rho-dependent signaling pathway. *J. Cell Biol.* 135, 37–51.
- Holmsen, H., and Dangelmaier, C.A. (1989). Measurement of secretion of adenine nucleotides. *Methods Enzymol.* 169, 195–205.
- Hope, M.J., Bally, M.B., Mayer, L.D., Janoff, A.S., and Cullis, P.R. (1986). Generation of multilamellar and unilamellar phospholipid vesicles. *Chem. Phys. Lipids* 40, 89–107.

- Huang, L., Wong, T.Y.W., Lin, R.W.W., and Furthmayr, H. (1999). Replacement of ⁵⁵⁸threonine, a critical site of phosphorylation of moesin *in vivo*, with aspartate activates F-actin binding of moesin: regulation of conformational change. *J. Biol. Chem.* *274*, 12803–12810.
- Igarashi, T. (1987). In: *Handbook of Surfactants*, ed. T. Yoshida, S. Shindo, T. Ohgaki and T. Yamanaka, Tokyo: Kogakusha, 116–139.
- Janmey, P.A. (1994). Phosphoinositides and calcium as regulators of cellular actin assembly and disassembly. *Annu. Rev. Physiol.* *56*, 169–191.
- Johnson, R.P., and Craig, S.W. (1994). F-actin binding site masked by the intramolecular association of vinculin head and tail domains. *Nature* *373*, 261–264.
- Johnson, R.P., and Craig, S.W. (1995). An intramolecular association between the head and tail domains of vinculin modulates talin binding. *J. Biol. Chem.* *269*, 12611–12619.
- Joust, B., and Rudiger, M. (1998). Crosstalk between cell adhesion molecules: vinculin as a paradigm for regulation by conformation. *Trends Cell Biol.* *6*, 311–315.
- Kaibuchi, K., Takai, Y., Sawamura, M., Hoshijima, M., Fujikura, T., and Nishizuka, Y. (1983). Synergistic functions of protein phosphorylation and calcium mobilization in platelet activation. *J. Biol. Chem.* *258*, 6701–6704.
- King, M.D., and Marsh, D. (1987). Head group and chain length dependence of phospholipid self-assembly studied by spin-label electron spin resonance. *Biochemistry* *26*, 1224–1231.
- Kotani, H., Takaishi, K., Sasaki, T., and Takai, Y. (1997). Rho regulates association of both the ERM family and vinculin with the plasma membrane in MDCK cells. *Oncogene* *14*, 1705–1713.
- Krieg, J., and Hunter, T. (1992). Identification of the two major epidermal growth factor-induced tyrosine phosphorylation sites in the microvillar core protein ezrin. *J. Biol. Chem.* *267*, 19258–19265.
- Kyte, J., and Doolittle, R.F. (1982). A method for displaying the hydrophathic character of a protein. *J. Mol. Biol.* *157*, 105–132.
- Lamb, R.F., Ozanne, B.W., Roy, C., McGarry, L., Stipp, C., Mangeat, P., and Jay, D.G. (1997). Essential functions of ezrin in maintenance of cell shape and lamellipodial extension in normal and transformed fibroblasts. *Curr. Biol.* *7*, 682–688.
- Lankes, W., Griesmacher, A., Gruenwald, J., Schwartz-Albiez, R., and Keller, R. (1988). A heparin-binding protein involved in inhibition of smooth muscle cell proliferation. *Eur. J. Biochem.* *251*, 831–842.
- Lankes, W., Schwartz-Albiez, R., and Furthmayr, H. (1993). Cloning and sequencing of porcine moesin and radixin cDNA and identification of highly conserved domains. *Biochim. Biophys. Acta* *1216*, 479–482.
- Lankes, W.T., and Furthmayr, H. (1991). Moesin: a member of the protein 4.1-talin-ezrin family of proteins. *Proc. Natl. Acad. Sci. USA* *88*, 8297–8301.
- Legg, J.W., and Isacke, C.M. (1998). Identification and functional analysis of the ezrin-binding site in the hyaluran receptor, CD44. *Curr. Biol.* *8*, 705–708.
- Lipfert, L., Haimovich, B., Schaller, M.D., Cobb, B.S., Parsons, J.T., and Brugge, J.S. (1992). Integrin-dependent phosphorylation and activation of the protein tyrosine kinase pp125FAK in platelets. *J. Cell Biol.* *119*, 905–912.
- Lu, P.J., and Chen, C.S. (1997). Selective recognition of phosphatidylinositol 3,4,5-triphosphate by a synthetic peptide. *J. Biol. Chem.* *272*, 466–472.
- Mackay, D.J.G., Esch, F., Furthmayr, H., and Hall, A. (1997). Rho and rac-dependent assembly of focal adhesion complexes and actin filaments in permeabilized fibroblasts: an essential role for ERM proteins. *J. Cell Biol.* *138*, 927–938.
- Machesky, L.M., and Hall, A. (1997). Role of actin polymerization and adhesion to extracellular matrix in rac- and rho-induced cytoskeletal reorganization. *J. Cell Biol.* *138*, 913–926.
- Magendantz, M., Henry, M.D., Lander, A., and Solomon, F. (1995). Interdomain interactions of radixin *in vitro*. *J. Biol. Chem.* *270*, 25324–25327.
- Matsui, T., Amano, M., Yamamoto, T., Chihara, K., Nakafuku, M., Ito, M., Nakano, T., Okawa, K., Iwamatsu, A., and Kaibuchi, K. (1996). Rho-associated kinase, a novel serine-threonine kinase, is a putative target for small GTP-binding protein rho. *EMBO J.* *15*, 2208–2216.
- Matsui, T., Maeda, M., Doi, Y., Yonemura, S., Amano, M., Kaibuchi, K., Tsukita, S., and Tsukita, S. (1998). Rho-kinase phosphorylates COOH-terminal threonines of ezrin/radixin/moesin (ERM) proteins and regulates their head-to-tail association. *J. Cell Biol.* *140*, 647–657.
- Meyer, T., Regenass, U., Fabbro, D., Alteri, E., Rosel, J., Muller, M., Caravatti, G., and Matter, A. (1989). A derivative of staurosporine (CGP 41 251) shows selectivity for protein kinase C inhibition and *in vitro* anti-proliferative as well as *in vivo* anti-tumor activity. *Int. J. Cancer* *43*, 851–856.
- Mitchison, T., and Kirschner, M. (1988). Cytoskeletal dynamics and Nerve Growth. *Neuron* *1*, 761–822.
- Murphy, C.T., and Westwick, J. (1994). Role of type 1 and type 2A phosphatases in signal transduction of platelet-activating-factor-stimulated rabbit platelets. *Biochem. J.* *301*, 531–537.
- Nakamura, F., Amieva, M.R., and Furthmayr, H. (1995). Phosphorylation of threonine 558 in the carboxyl-terminal actin-binding domain of moesin by thrombin activation of human platelets. *J. Biol. Chem.* *270*, 31377–31385.
- Nakamura, F., Amieva, M.R., Hirota, C., Mizuno, Y., and Furthmayr, H. (1996). Phosphorylation of 558T of moesin detected by site-specific antibodies in RAW264.7 macrophages. *Biochem. Biophys. Res. Commun.* *226*, 650–656.
- Nakano, H., Kobayashi, E., Takahashi, I., Tamaoki, T., Kuzuu, Y., and Iba, H. (1987). Staurosporine inhibits tyrosine-specific protein kinase activity of Rous sarcoma virus transforming protein p60. *J. Antibiot.* *40*, 706–708.
- Niggli, V., Andreoli, C., Roy, C., and Mangeat, P. (1995). Identification of a phosphatidylinositol-4,5-bisphosphate-binding domain in the N-terminal region of ezrin. *FEBS Lett.* *376*, 172–176.
- Packham, M.A. (1994). Role of platelets in thrombosis and hemostasis. *Can. J. Physiol. Pharmacol.* *72*, 278–284.
- Paglini, G., Kunda, P., Quiroga, S., Kosik, K., and Caceras, A. (1998). Suppression of radixin and moesin alters growth cone morphology, motility, and process formation in primary cultured neurons. *J. Cell Biol.* *143*, 443–455.
- Pearson, M., Reczek, D., Bretscher, A., and Karplus, P.A. (1998). Crystallographic studies of moesin: a protein that links the actin cytoskeleton to the plasma membrane. *Mol. Biol. Cell* *9*, 265a (Abstract).
- Pedrotti, B., Colombo, R., and Islam, K. (1994). Microtubule associated protein MAP1A is an actin-binding and cross-linking protein. *Cell Motil. Cytoskeleton* *29*, 110–116.
- Pestonjampasp, K., Amieva, M.R., Strassel, C.P., Nauseef, W.M., Furthmayr, H., and Luna, E.J. (1995). Moesin, ezrin, and p205 are actin-binding proteins associated with neutrophil plasma membranes. *Mol. Biol. Cell* *6*, 247–259.

- Pietromonaco, S.F., Simons, P.C., Altman, A., and Elias, L. (1998). Protein kinase C-theta phosphorylation of moesin in the actin-binding sequence. *J. Biol. Chem.* *273*, 7594–7603.
- Ragunathan, V., Mowery, P., Rozycki, M., Lindberg, U., and Schutt, C. (1992). Structural changes in profilin accompany its binding to phosphatidylinositol 4,5-bisphosphate. *FEBS Lett.* *297*, 46–50.
- Reczek, D., Berryman, M., and Bretscher, A. (1997). Identification of EBP50: a PDZ-containing phosphoprotein that associates with members of the ezrin-radixin-moesin family. *J. Cell Biol.* *139*, 169–179.
- Roy, C., Martin, M., and Mangeat, P. (1997). A dual involvement of the amino-terminal domain of ezrin in F- and G-actin binding. *J. Biol. Chem.* *272*, 20088–20095.
- Sah, V.P., Hoshijima, M., Chien, K.R., and Brown, J.H. (1996). Rho is required for alpha₁ and alpha₁-adrenergic receptor signaling in cardiomyocytes. Dissociation of Ras and Rho pathways. *J. Biol. Chem.* *271*, 31185–31190.
- Sano, K., Takai, Y., Yamanishi, J., and Nishizuka, Y. (1983). A role of calcium-activated phospholipid-dependent protein kinase in human platelet activation. Comparison of thrombin and collagen actions. *J. Biol. Chem.* *258*, 2010–2013.
- Schoenwaelder, S.M., Jackson, S.P., Yuan, Y., Teasdale, M.S., Salem, H.H., and Mitchell, C.A. (1994). Tyrosine kinases regulate the cytoskeletal attachment of integrin alpha IIb beta 3 (platelet glycoprotein IIb/IIIa) and the cellular retraction of fibrin polymers. *J. Biol. Chem.* *269*, 32479–32487.
- Serrador, J.M., Alonso-Lebrero, J.L., del Pozo, M.A., Furthmayr, H., Schwartz-Albiez, R., Calvo, J., Lozano, F., and Sanchez-Madrid, F. (1997). Moesin interacts with the cytoplasmic region of intercellular adhesion molecule-3 and is redistributed to the uropod of T-lymphocytes during cell polarization. *J. Cell Biol.* *138*, 1409–1423.
- Shaw, R.J., Henry, M., Solomon, F., and Jacks, T. (1998). RhoA-dependent phosphorylation and relocalization of ERM proteins into apical membrane/actin protrusions in fibroblasts. *Mol. Biol. Cell* *9*, 403–419.
- Short, D.B., Trotter, K.W., Reczek, D., Kreda, S.M., Bretscher, A., Boucher, R.C., Stutts, M.J., and Milgram, S.L. (1998). An apical PDZ protein anchors the cystic fibrosis transmembrane conductance regulator to the cytoskeleton. *J. Biol. Chem.* *273*, 19797–19801.
- Simons, P.C., Pietromonaco, S.F., Reczek, D., Bretscher, A., and Elias, L. (1998). C-terminal threonine phosphorylation activates ERM proteins to link the cells' cortical lipid bilayer. *Biochem. Biophys. Res. Commun.* *253*, 561–565.
- Spudich, J.A., and Watt, S. (1971). The regulation of rabbit skeletal muscle contraction. I. Biochemical studies of the interaction of the tropomyosin-troponin complex with actin and the proteolytic fragments of myosin. *J. Biol. Chem.* *246*, 4866–4871.
- Supattopone, S., Worley, P.F., Baraban, J.M., and Snyder, S.H. (1988). Solubilization, purification, and characterization of an inositol triphosphate receptor. *J. Biol. Chem.* *263*, 1530–1534.
- Takeda, H., Nagafuchi, A., Yonemura, S., Tsukita, S., Behrens, J., Birchmeier, W., and Tsukita, S. (1995). V-src kinase shifts the cadherin-based cell adhesion from the strong to the weak state and beta catenin is not required for the shift. *J. Cell Biol.* *131*, 1839–1847.
- Takeuchi, K., Sato, N., Kasahara, H., Funayama, N., Nagafuchi, A., Yonemura, S., Tsukita, S., and Tsukita, S. (1994). Perturbation of cell adhesion and microvilli formation by antisense oligonucleotides to ERM family members. *J. Cell Biol.* *125*, 1371–1384.
- Thompson, W., and MacDonald, G. (1976). Cytidine diphosphate diglyceride of bovine brain. Positional distribution of fatty acids and analysis of major molecular species. *Eur. J. Biochem.* *65*, 107–111.
- Torti, M., Ramaschi, G., Sinigaglia, F., Lapetina, E.G., and Balduini, C. (1994). Glycoprotein IIb-IIIa and the translocation of Rap2B to the platelet cytoskeleton. *Proc. Natl. Acad. Sci. USA* *91*, 4239–4243.
- Tsukita, S., Hieda, Y., and Tsukita, S. (1989). A new 82-kD barbed end-capping protein (radixin) localized in the cell-to-cell adherens junction: purification and characterization. *J. Cell Biol.* *108*, 2369–2382.
- Turunen, O., Wahlstrom, T., and Vaheri, A. (1994). Ezrin has a COOH-terminal actin-binding site that is conserved in the ezrin protein family. *J. Cell Biol.* *126*, 1445–1453.
- Urushidani, T., Hanzel, D.K., and Forte, J.G. (1989). Characterization of an 80-kDA phosphoprotein involved in parietal cell stimulation. *Am. J. Physiol.* *256*, 1070–1081.
- Yao, X., Cheng, L., and Forte, J.G. (1996). Biochemical characterization of ezrin-actin interaction. *J. Biol. Chem.* *271*, 7224–7229.
- Yonemura, S., Nagafuchi, A., Sato, N., and Tsukita, S. (1993). Concentration of an integral membrane protein, CD43 (leukosialin, sialophorin), in the cleavage furrow through the interaction of its cytoplasmic domain with actin-based cytoskeletons. *J. Cell Biol.* *120*, 437–449.
- Zhang, J., King, W.G., Dillon, S., Hall, A., Feig, L., and Rittenhouse, S.E. (1993). Activation of platelet phosphatidylinositol 3-kinase requires the small GTP-binding protein Rho. *J. Biol. Chem.* *268*, 22251–22254.
- Zhang, Q., Magnusson, M.K., and Mosher, D.F. (1997). Lysophosphatidic acid and microtubule-destabilizing agents stimulate fibronectin matrix assembly through rho-dependent actin stress fiber formation and cell contraction. *Mol. Biol. Cell* *8*, 1415–1425.